Article

Isomeric Forms of Heavier Main Group Hydrides: Experimental and Theoretical Studies of the [Sn(Ar)H] (Ar = Terphenyl) System

Eric Rivard, Roland C. Fischer, Robert Wolf, Yang Peng, W. Alexander Merrill, Nathan D. Schley, Zhongliang Zhu, Lihung Pu, James C. Fettinger, Simon J. Teat, Isreal Nowik, Rolfe H. Herber, Nozomi Takagi, Shigeru Nagase, and Philip P. Power

J. Am. Chem. Soc., **2007**, 129 (51), 16197-16208 • DOI: 10.1021/ja076453m

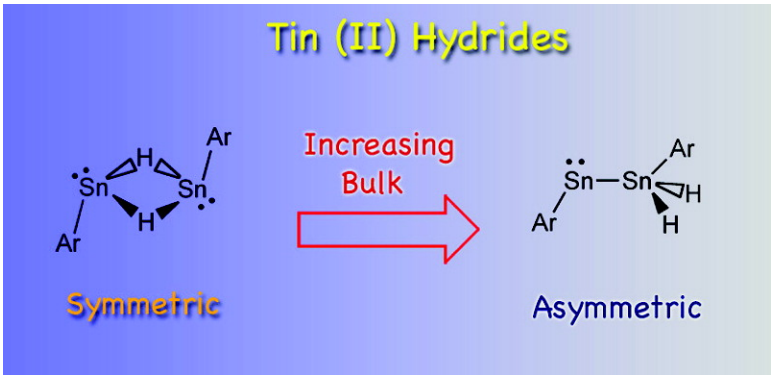

More About This Article

Additional resources and features associated with this article are available within the HTML version:

- Supporting Information
- Links to the 4 articles that cite this article, as of the time of this article download
- Access to high resolution figures
- Links to articles and content related to this article
- Copyright permission to reproduce figures and/or text from this article

View the Full Text HTML

J|A|C|S
ARTICLES
Published on Web 12/04/2007

Isomeric Forms of Heavier Main Group Hydrides: Experimental and Theoretical Studies of the $[Sn(Ar)H]_2$ (Ar = Terphenyl) System

Eric Rivard,[†] Roland C. Fischer,[†] Robert Wolf,[†] Yang Peng,[†] W. Alexander Merrill,[†] Nathan D. Schley,[†] Zhongliang Zhu,[†] Lihung Pu,[‡] James C. Fettinger,[†] Simon J. Teat,[§] Isreal Nowik,[||] Rolfe H. Herber,*[,||] Nozomi Takagi,[⊥] Shigeru Nagase,*[,⊥] and Philip P. Power*[,†]

Department of Chemistry, University of California, Davis, One Shields Avenue, Davis, California, 95616, Department of Chemistry, California State University, Dominguez Hills, 1000 East Victoria Street, Carson, California, 90747, Advanced Light Source, Lawrence Berkeley Laboratory, One Cyclotron Road, MS2-400, Berkeley, California, 94720, Racah Institute of Physics, Hebrew University of Jerusalem, 91904, Jerusalem, Israel, and Department of Theoretical and Computational Molecular Science, Institute for Molecular Science, Okazaki, Aichi 444-8585, Japan

Received August 31, 2007; E-mail: pppower@ucdavis.edu

Abstract: A series of symmetric divalent Sn(II) hydrides of the general form $[(4\text{-X}-\text{Ar}')\text{Sn}(\mu\text{-H})]_2$ (4-X−Ar′ = C_6H_2-4-X-2,6-(C_6H_3-2,6-^{i}Pr$_2$)$_2$; X = H, MeO, ^{t}Bu, and $SiMe_3$; **2**, **6**, **10**, and **14**), along with the more hindered asymmetric tin hydride (3,5-^{t}Pr$_2$−Ar*)SnSn(H)$_2$(3,5-^{i}Pr$_2$−Ar*) (**16**) (3,5-^{t}Pr$_2$−Ar* = 3,5-^{i}Pr$_2$−C_6H-2,6-(C_6H_2-2,4,6-^{i}Pr$_3$)$_2$), have been isolated and characterized. They were prepared either by direct reduction of the corresponding aryltin(II) chloride precursors, ArSnCl, with $LiBH_4$ or ^{i}Bu$_2$AlH (DIBAL), or via a transmetallation reaction between an aryltin(II) amide, $ArSnNMe_2$, and BH_3·THF. Compounds **2**, **6**, **10**, and **14** were obtained as orange solids and have centrosymmetric dimeric structures in the solid state with long Sn···Sn separations of 3.05 to 3.13 Å. The more hindered tin(II) hydride **16** crystallized as a deep-blue solid with an unusual, formally mixed-valent structure wherein a long Sn−Sn bond is present [Sn−Sn = 2.9157(10) Å] and two hydrogen atoms are bound to one of the tin atoms. The Sn−H hydrogen atoms in **16** could not be located by X-ray crystallography, but complementary Mössbauer studies established the presence of divalent and tetravalent tin centers in **16**. Spectroscopic studies (IR, UV−vis, and NMR) show that, in solution, compounds **2**, **6**, **10**, and **14** are predominantly dimeric with Sn−H−Sn bridges. In contrast, the more hindered hydrides **16** and previously reported $(Ar^*SnH)_2$ (**17**) (Ar* = C_6H_3-2,6-(C_6H_2-2,4,6-^{i}Pr$_3$)$_2$) adopt primarily the unsymmetric structure $ArSnSn(H)_2Ar$ in solution. Detailed theoretical calculations have been performed which include calculated UV−vis and IR spectra of various possible isomers of the reported hydrides and relevant model species. These showed that increased steric hindrance favors the asymmetric form $ArSnSn(H)_2Ar$ relative to the centrosymmetric isomer $[ArSn(\mu\text{-H})]_2$ as a result of the widening of the interligand angles at tin, which lowers steric repulsion between the terphenyl ligands.

Introduction

Until recently, examples of stable organotin hydrides were confined to the +4 oxidation state, where di- and triorganotin hydrides R_2SnH_2 and R_3SnH are important for a rich variety of chemical transformations.[1] For example, tri-*n*-butyltin hydride is a widely used reducing agent in organic and inorganic chemistry,[2] and this versatile species mediates many radical-driven organic reactions.[3] Furthermore, diorganotin dihydrides have been used as precursors for a variety of novel heteroaromatic ring systems including borato- and phosphabenzenes.[4] Under suitable conditions, dehydrocoupling polymerization of alkylated stannanes, R_2SnH_2, can be induced to yield polystannanes $(R_2Sn)_n$ which exhibit interesting electronic properties.[5]

In 2000, the synthesis of $(Ar^*SnH)_2$, Ar* = C_6H_3-2,6-(C_6H_2-2,4,6-^{i}Pr$_3$)$_2$, the first example of a divalent tin(II) hydride stable at ambient temperature, was reported.[6] This discovery was made

[†] University of California.
[‡] California State University.
[§] Lawrence Berkeley Laboratory.
[||] Hebrew University of Jerusalem.
[⊥] Institute for Molecular Science.

(1) (a) Davies, A. G. *Organotin Chemistry*; VCH: New York, 1997. (b) Pereyre, M.; Quintand, J.-P.; Rahm, A. *Tin in Organic Synthesis*; Butterworth: London, 1987.
(2) (a) Chen, L.; Cotton, F. A.; Wojtczak, W. A. *Inorg. Chim. Acta* **1996**, *252*, 239. (b) Neumann, W. P. *Synthesis* **1987**, 665. (c) Giese, B. *Radicals in Organic Synthesis: Formation of Carbon-Carbon Bonds*; Pergamon Press: Oxford 1986.
(3) (a) Curran, D. P. *Synthesis* **1988**, 417. (b) Kuivila, H. G. *Acc. Chem. Res.* **1968**, *1*, 299.
(4) (a) Fu, G. C. *Adv. Organomet. Chem.* **2001**, *47*, 101. (b) Ashe, A. J. *Acc. Chem. Res.* **1978**, *11*, 153. (c) Emslie, D. J. H.; Piers, W. E.; Parvez, M. *Angew. Chem., Int. Ed.* **2003**, *42*, 1252.
(5) Imori, T.; Tilley, T. D. *J. Chem. Soc., Chem. Commun.* **1993**, 1607.

Chart 1. Possible Isomeric Forms for Sn_2H_4

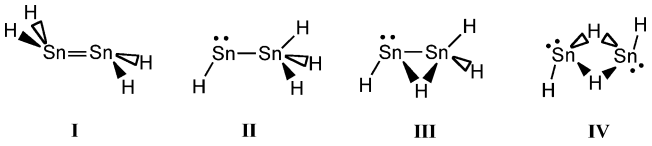

I II III IV

possible by the introduction of a bulky terphenyl ligand at tin which sterically protects the reactive Sn−H moiety from degradation processes. More recently Roesky and co-workers prepared a terminal Sn(II) hydride that was stabilized by a β-diketiminate ligand.[7]

Theoretical studies on lower oxidation state group 14 hydrides have focused on the relative stability of monomeric EH_2 (E = group 14 element) and the dimeric forms as illustrated by the tin derivatives in Chart 1.[8,9] Trinquier has calculated the energies of the heavier congeners of ethylene $H_2E{=}EH_2$ (E = Si, Ge, Sn and Pb) as well as the isomeric forms shown in Chart 1.[8] In the case of carbon, the planar (D_{2h}) ethylene isomer is by far the most stable form with the asymmetric structure analogous to **II** lying over 70 kcal/mol higher in energy. This picture is drastically altered in the heavier congeners and for the four tin isomers **I**−**IV** where the energy spread is only about 10 kcal/mol, with the hydride-bridged isomer **IV** being the most stable. Interestingly, Trinquier also showed that the asymmetric, mixed-valent species $HSn{-}SnH_3$ (**II**) was only slightly less stable than the hydride-bridged dimer **IV** by 1.3 to 7 kcal/mol (depending on the calculation method used).[8] This work suggested that, for tin(II) hydrides $(RSnH)_2$ containing a stabilizing bulky group (R), the isomeric forms analogous to those presented in Chart 1 might have similar relative energies, and hence representative examples of each structure type could be accessible.[10,11]

Parallel work on terphenyl stabilized Sn−Sn multiple bonded complexes has shown that their structures could be altered by changing the electronic and steric properties of the terphenyl group.[12] We now report the synthesis and characterization of a range of Sn(II) hydrides and show that modification of the terphenyl ligand produces different structural types.[13] In addition, a combined theoretical and experimental approach is used to explain why, in some instances, centrosymmetric structures such as **IV** are formed, while, in others, the asymmetric form related to **II** is favored.

Experimental Section

All reactions were performed with the use of modified Schlenk techniques under an atmosphere of nitrogen or in a Vacuum Atmospheres Nexus Drybox. Solvents were dried and collected using a Grubbs-type[14] solvent purification system manufactured by Glass Contour and degassed twice (freeze−pump−thaw method) prior to use. [4-H−Ar′]Li (4-H−Ar′ = Ar′ = C_6H_3-2,6-(C_6H_3-2,6-$^iPr_2$)$_2$),[15] (Ar′-SnCl)$_2$,[12] and [3,5-$^iPr_2$−Ar*]Li (3,5-$^iPr_2$−Ar* = 3,5-$^iPr_2$−C_6H-2,6-(C_6H_2-2,4,6-$^iPr_3$)$_2$),[16] were prepared according to literature procedures. 1-Iodo-2,6-dibromo-4-*tert*-butylbenzene[17] and 2,6-dichloro-4-trimethylsilylbenzene[18] were also synthesized as described in the literature. ^{n}BuLi (2.5 M solution in hexanes), anhydrous $SnCl_2$, $LiBH_4$, $LiNMe_2$, $^iBu_2$AlH (DIBAL), BH_3·THF (1.0 M solution in THF), and 3,5-dichloroanisole were purchased from commercial sources and used as received. The syntheses of 4-MeO−Ar′I (**3**), 4-^{t}Bu−Ar′I (**7**), 4-Me_3Si−Ar′I (**11**), and their respective lithium salts (**4**, **8**, and **12**) were carried out in an analogous manner to that for the syntheses of Ar′I and Ar′Li;[15] full details are given in the Supporting Information. ^{1}H and ^{13}C{^{1}H} NMR spectra were obtained on a Varian Mercury 300 MHz spectrometer (300.1 and 75.5 MHz, respectively) and referenced internally to residual protio benzene or chloroform in the C_6D_6 or $CDCl_3$ solvent. Solution ^{29}Si and ^{119}Sn NMR spectra were recorded on a Varian Inova 600 MHz spectrometer (119.2 and 224.2 MHz, respectively) and referenced externally to neat $SiMe_4$ or $SnMe_4$. Infrared spectra were recorded as Nujol mulls between CsI plates using a Perkin-Elmer 1430 instrument, while UV−vis data were collected on a Hitachi-1200 instrument. Melting points were obtained in sealed glass capillaries under nitrogen using a Mel-Temp II apparatus and are uncorrected.

^{119}Sn Mössbauer Effect Spectroscopy. Temperature-dependent Mössbauer experiments were carried out in transmission mode[19] using an ~5 mCi source of ^{119}Sn in a $BaSnO_3$ matrix. Spectroscopic calibration was accomplished by using a 20 mg·cm^{-2} α-Fe absorber at room temperature (^{57}Co in Rh source). Isomer shifts are reported with respect to the centroid of the room-temperature $BaSnO_3$ spectrum. The samples were transferred in an inert atmosphere glovebox to O-ring-sealed plastic sample holders and immediately cooled to liquid nitrogen temperature. They were then transferred to a precooled cryostat and examined in transmission geometry. All temperature-dependent Mössbauer data were obtained in both warming and cooling modes, and no evidence of hysteresis was observed. It was noted that **2** is strongly photochromic. A sealed sample of **2** was exposed to strong sunlight for *ca.* 5 min and found to have changed color from orange to green. A rapidly cooled sample of the green form was examined by Mössbauer spectroscopy at 90 K and found to retain the same hyperfine parameters (IS and QS) as the orange form, as detailed below (Table 3). On warming the green form to room temperature the orange color slowly returned and was complete after *ca.* 30 min.

X-ray Crystallography. Crystals of appropriate quality for X-ray diffraction studies were removed from a Schlenk tube under a stream of nitrogen and immediately covered with a thin layer of hydrocarbon oil (Paratone). A suitable crystal was then selected and attached to a glass fiber and quickly placed in a low-temperature stream of nitrogen (90(2) K).[20] Data for compound **2**[13] were obtained on a Bruker SMART 1000 instrument using Mo Kα radiation (λ = 0.710 73 Å) in conjunction with a CCD detector; data for compounds **6**, **10**, and **14** were similarly obtained using a Bruker APEX II instrument. The collected reflections were corrected for Lorentz and polarization effects by using Blessing's method as incorporated into the program SADABS.[21,22] The structures

(6) Eichler, B. E.; Power, P. P. *J. Am. Chem. Soc.* **2000**, *122*, 8785.
(7) Pineda, L. W.; Jancik, V.; Starke, K.; Oswald, R. B.; Roesky, H. W. *Angew. Chem., Int. Ed.* **2006**, *45*, 2602.
(8) (a) Trinquier, G. *J. Am. Chem. Soc.* **1991**, *113*, 144. (b) Balasubramanian, K. *J. Chem. Phys.* **1988**, *89*, 5731.
(9) SnH_2 has been prepared and characterized in an argon matrix, see: Wang, X.; Andrews, L.; Chertihin, G. V.; Souter, P. F. *J. Phys. Chem. A* **2002**, *106*, 6302.
(10) (a) Lappert, M. F. *Main Group Met. Chem.* **1994**, *17*, 114. (b) Stanciu, C.; Richards, A. F.; Power, P. P. *J. Am. Chem. Soc.* **2004**, *126*, 4106. (c) Lee, V. Ya; Fukawa, T.; Nakamoto, M.; Sekiguchi, A.; Tumanskii, B. L.; Kami, M.; Apeloig, Y. *J. Am. Chem. Soc.* **2006**, *128*, 11643.
(11) Ge(II) hydrides have also been prepared; see: (a) Ding, Y.; Roesky, H. W.; Noltemeyer, M.; Schmidt, H.-G.; Power, P. P. *Organometallics* **2001**, *20*, 1190. (b) Richards, A. F.; Phillips, A. D.; Olmstead, M. M.; Power, P. P. *J. Am. Chem. Soc.* **2003**, *125*, 3204. (c) Spikes, G. H.; Fettinger, J. C.; Power, P. P. *J. Am. Chem. Soc.* **2005**, *127*, 12232. (d) See ref 7.
(12) Pu, L.; Phillips, A. D.; Richards, A. F.; Stender, M.; Simons, R. S.; Olmstead, M. M.; Power, P. P. *J. Am. Chem. Soc.* **2003**, *125*, 11626.
(13) Rivard, E.; Steiner, J.; Fettinger, J. C.; Giuliani, J. R.; Augustine, M. P.; Power, P. P. *Chem. Commun.* **2007**, 4919.
(14) Pangborn, A. B.; Giardello, M. A.; Grubbs, R. H.; Rosen, R. K.; Timmers, F. J. *Organometallics* **1996**, *15*, 1518.
(15) Schiemenz, B.; Power, P. P. *Angew. Chem., Int. Ed. Engl.* **1996**, *35*, 2150.
(16) Stanciu, C.; Richards, A. F.; Fettinger, J. C.; Brynda, M.; Power, P. P. *J. Organomet. Chem.* **2006**, *691*, 2540.
(17) (a) Craig, D. *J. Am. Chem. Soc.* **1935**, *57*, 195. (b) Drake, N. L.; Eaker, C. M.; Garman, J. A.; Hamlin, K. E., Jr.; Hayes, R. A.; Haywood, S. T.; Peck, R. M.; Preston, R. K.; Sterling, J., Jr.; van Hook, J. O.; Walton, E. *J. Am. Chem. Soc.* **1946**, *68*, 1602. (c) Bedard, T. C.; Moore, J. S. *J. Am. Chem. Soc.* **1995**, *117*, 10662.
(18) Wrobel, D.; Wannagat, U. *J. Organomet. Chem.* **1982**, *225*, 203.
(19) Adams, R. D.; Captain, B.; Herber, R. H.; Johansson, M.; Nowik, I.; Smith, J. L., Jr.; Smith, M. D. *Inorg. Chem.* **2005**, *44*, 6346.
(20) Hope, H. *Prog. Inorg. Chem.* **1995**, *41*, 1.
(21) Blessing, R. H. *Acta Crystallogr.* **1995**, *51A*, 33.

Table 1. Selected Crystallographic Data for Compounds **2**, **6**, **10**, **14**, and **16**

	2	**6**	**10**	**14**	**16**
formula	$C_{60}H_{76}Sn_2$	$C_{74}H_{92}O_2Sn_2$	$C_{80}H_{104}Sn_2$	$C_{70}H_{102}OSi_2Sn_2$	$C_{87}H_{131}Sn_2$
fw	1034.59	1250.86	1303.01	1253.08	1414.30
color, habit	orange, block	yellow, plate	orange, block	orange, block	blue, needle
cryst syst	triclinic	orthorhombic	monoclinic	monoclinic	tetragonal
space group	$P\bar{1}$	$Pna2_1$	$P2_1/n$	$P2_1/c$	$P4_2/n$
a, Å	9.2996(16)	15.8356(8)	17.488(3)	11.4360(7)	33.9416(13)
b, Å	12.814(2)	15.1379(8)	11.6926(17)	25.5484(15)	33.9416(13)
c, Å	12.938(2)	26.5935(14)	17.666(3)	12.8457(7)	14.7839(12)
α, deg	110.141(3)	90	90	90	90
β, deg	98.399(3)	90	94.351(3)	114.7570(10)	90
γ, deg	110.940(3)	90	90	90	90
V, Å^3	1286.6(4)	6374.9(6)	3602.1(9)	3408.2(3)	17031.5(17)
Z	1	4	2	2	8
cryst dim, mm^3	0.12 × 0.11 × 0.03	0.29 × 0.22 × 0.08	0.19 × 0.16 × 0.12	0.39 × 0.31 × 0.20	0.15 × 0.04 × 0.01
d_{calc}, g cm^{-3}	1.335	1.303	1.201	1.221	1.103
μ, mm^{-1}	1.007	0.828	0.733	0.806	0.775
no. of reflns	4677	51658	6492	43294	123148
no. of obsd reflns	3674	12337	4418	6457	11248
no. of param	293	741	386	386	839
R_1 obsd reflns	0.0554	0.0425	0.0674	0.0327	0.0679
wR_2, all	0.1658	0.1058	0.1870	0.0868	0.1956

were solved by direct methods and refined with the SHELXTL v.6.1 software package.[23] Refinement was by full-matrix least-squares procedures with all carbon-bound hydrogen atoms included in calculated positions and treated as riding atoms.

X-ray crystallographic data for **16** were collected at the ALS Synchrotron facility at UC Berkeley on a Bruker Platinum 300 diffractometer at 80(2) K using monochromated synchrotron radiation (λ = 0.774 90 Å). Absorption corrections were performed using SADABS.[21,22] The structure was solved by the Patterson method, and all non-hydrogen atoms were refined anisotropically with the exception of some (five out of 15) ^{i}Pr groups within the 3,5-^{i}Pr$_2$−Ar* ligand. These disordered groups were either refined as a whole with isotropic atomic displacement parameters, or in two cases, their methyl groups were refined in split positions with isotropic atomic displacement parameters. Furthermore, the structure contained an *n*-hexane solvent molecule that was strongly disordered over a crystallographic inversion center. SADI constraints were used to obtain a reasonable geometry. However the thermal parameters remained quite high, and isotropic atomic displacement parameters were used. Due to the observed disorder and the weakly diffracting nature of the selected crystal, the structure is only of modest quality and, consequently, the two hydrogen atoms next to Sn(1) could not be located on the Fourier difference map. Relevant crystallographic and structural refinement parameters are listed in Table 1.

Theoretical Calculations. All calculations were conducted using the Gaussian 03 series of electronic structure programs.[24] The geometries were optimized with the density functional theory at the B3PW91 level.[25] The [4333111/433111/43] basis set augmented by two d polarization functions (d exponents 0.253 and 0.078) was used for Sn, while the 6-31G(d) basis set was used for C and H.[26]

Syntheses. Preparation of Ar′SnNMe$_2$ (1). To a solution of Ar′SnCl (1.69 g, 3.07 mmol) in 35 mL of Et$_2$O was added dropwise a slurry of LiNMe$_2$ (0.160 g, 3.11 mmol) in 25 mL of Et$_2$O. The reaction was stirred for 16 h to give a deep yellow solution along with a white precipitate. The mixture was then filtered through Celite, and the solvent was removed to give a bright yellow solid. Recrystallization of this product from 15 mL of hexanes (*ca.* −20 °C) afforded **1** as yellow blade-shaped crystals (1.40 g, 82%). Mp (°C): 106−108 (dec). UV−vis (hexanes) λ_{max} [nm] (ϵ in M^{-1} cm^{-1}): 370 (shoulder). ^{1}H NMR (C$_6$D$_6$): δ 7.30 (t, 2H, J = 7.5 Hz, Ar*H*), 7.15−7.22 (m, 7H, Ar*H*), 3.18 (septet, 4H, $^3J_{HH}$ = 6.9 Hz, C*H*(CH$_3$)$_2$), 3.03 (s, 6H, N(C*H*$_3$)$_2$), 1.33 (d, 12H, $^3J_{HH}$ = 6.6 Hz, CH(C*H*$_3$)$_2$), 1.08 (d, 12H, $^3J_{HH}$ = 6.6 Hz, CH(C*H*$_3$)$_2$). ^{13}C{^{1}H} NMR (C$_6$D$_6$): δ 177.6, 147.6, 146.9, 145.6, 138.8, 130.1, 129.0 and 123. 5 (Ar*C*), 47.7 (br, N(*C*H$_3$)$_2$), 31.0 (*C*H(CH$_3$)$_2$), 26.7 (CH(*C*H$_3$)$_2$), 23.1 (CH(*C*H$_3$)$_2$). ^{119}Sn{^{1}H} NMR (C$_6$D$_6$): δ 817.

Preparation of [Ar′Sn(μ-H)]$_2$ (2). *Route A*:[13] To a deep yellow solution of **1** (0.761 g, 1.36 mmol) in 15 mL of Et$_2$O was added dropwise BH$_3$·THF (1.40 mL, 1.0 M solution in THF, 1.40 mmol). A deep blue-green solution was obtained from which an orange microcrystalline solid precipitated. After 2 h, the resulting light green solution was decanted from the precipitate and the solid **2** was dried under vacuum (0.51 g, 74%). *Route B*: To a mixture of Ar′SnCl (1.14 g, 2.07 mmol) and LiBH$_4$ (0.060 g, 2.8 mmol) were added 25 mL of cold (0 °C) diethyl ether. The reaction was warmed to room temperature and stirred for 2 h to give a green-brown solution over a tan precipitate. The mixture was then filtered, and the solvent was removed to give an orange solid that was identified as **2** on the basis of NMR and UV−vis spectroscopy (0.61 g, 57%). Crystals of **2** that were suitable for an X-ray diffraction study (orange blocks) were grown from a benzene solution at *ca.* 7 °C. Mp (°C): 181−183 (dec). UV−vis (benzene) λ_{max} [nm] (ϵ in M^{-1} cm^{-1}): 595 (70). ^{1}H NMR (C$_6$D$_6$): δ 9.13 (s, 1H, $^1J_{Sn-H}$ = *ca.* 89 Hz, Sn-*H*), 7.30 (t, 2H, $^3J_{HH}$ = 7.5 Hz, Ar*H*), 7.10 (m, 3H, Ar*H*), 7.03 (d, 4H, $^3J_{HH}$ = 7.5 Hz, Ar*H*), 3.00 (overlapping septets, 4H, C*H*(CH$_3$)$_2$), 1.11 (d, 6H, $^3J_{HH}$ = 6.6 Hz, CH(C*H*$_3$)$_2$), 1.04 (d, 6H, $^3J_{HH}$ = 6.6 Hz, CH(C*H*$_3$)$_2$), 1.02 (d, 6H, $^3J_{HH}$ = 6.6 Hz, CH(C*H*$_3$)$_2$), 0.93 (d, 6H, $^3J_{HH}$ = 6.9 Hz, CH(C*H*$_3$)$_2$). ^{119}Sn NMR (C$_6$D$_6$): δ 657 (br, $\Delta\omega_{1/2}$ = *ca.* 270 Hz). IR (Nujol, cm^{-1}): The Sn−H stretching band is likely obscured by ligand vibrations. ^{119}Sn Mössbauer (90 K, mm s^{-1}): Isomer shift (IS) = 2.805(4); Quadrupolar Splitting (QS) = 2.992(4).

Preparation of (4-MeO−Ar′)SnCl (5). A solution of 4-MeO−Ar′Li (**4**) (2.74 g, 6.6 mmol) in 25 mL of Et$_2$O was added dropwise to a slurry of SnCl$_2$ (1.51 g, 8.0 mmol) in 30 mL of Et$_2$O kept at 0 °C. The reaction mixture was then allowed to warm to room temperature during

(22) Sheldrick, G. M. *SADABS, version 2.10, Siemens Area Detector Absorption Correction*; Universität Göttingen: Göttingen, Germany, 2003.
(23) Sheldrick, G. M. *SHELXTL, version 6.1*; Bruker AXS, Inc.: Madison, WI, 2002.
(24) Frisch, M. J., et al. *Gaussian 03*, revision C.01; Gaussian, Inc.: Wallingford, CT, 2004.
(25) (a) Becke, A. D. *Phys. Rev.* **1988**, *A38*, 3098. (b) Becke, A. D. *J. Chem. Phys.* **1993**, *98*, 5648. (c) Perdew, J. P.; Wang, Y. *Phys. Rev.* **1992**, *B45*, 13244.
(26) (a) Huzinaga, S.; Andzelm, J.; Klobukowski, M.; Radzio-Andzelm, E.; Sakai, Y.; Tatewaki, H. *Gaussian Basis Sets for Molecular Calculations*; Elsevier: Amsterdam, 1984. (b) Francl, M. N.; Pietro, W. J.; Hehre, W. J.; Binkey, J. S.; Gordon, M. S.; DeFrees, D. J.; Pople, J. A. *J. Chem. Phys.* **1982**, *77*, 3654.

which an orange color developed. After stirring for 12 h, the solvent was removed under reduced pressure, and the resulting orange powder was extracted with 40 mL of toluene and filtered. Storage of the solution at *ca.* −20 °C for 12 h afforded large orange crystals of (4-MeO−Ar′)SnCl (1.53 g, 40%). Mp (°C): 187−190 (dec). UV−vis (hexanes) λ_{max} [nm] (ϵ in M^{-1} cm^{-1}): 402 (730). ^{1}H NMR (C_6D_6): δ 7.10−7.25 (m, 6H, Ar*H*), 6.99 (s, 2H, Ar*H*), 3.36 (s, 3H, OCH_3), 3.18 (septet, 4H, $^3J_{HH}$ = 6.9 Hz, C*H*(CH_3)$_2$), 1.31 (d, 12H, $^3J_{HH}$ = 6.6 Hz, CH(CH_3)$_2$), 1.03 (d, 12H, $^3J_{HH}$ = 6.6 Hz, CH(CH_3)$_2$). ^{13}C{^{1}H} NMR (C_6D_6): δ 159.6, 147.5, 146.7, 137.0, 129.2, 125.5, 123.7 and 116.5 (Ar*C*), 54.4 (O*C*H$_3$), 30.9 (*C*H(CH$_3$)$_2$), 26.4 (CH(*C*H$_3$)$_2$), 23.0 (CH(*C*H$_3$)$_2$). Attempts to obtain a ^{119}Sn NMR spectrum have been unsuccessful to date.

Synthesis of [(4-MeO−Ar′)Sn(μ-H)]$_2$ (6). Diethyl ether (50 mL) was added to a rapidly stirring mixture of **5** (1.00 g, 1.72 mmol) and $LiBH_4$ (0.045 g, 2.1 mmol) at 0 °C. After a few minutes, an orange precipitate was observed and the initially orange solution became yellow-green. The reaction was stirred for 1 h, and the precipitate was allowed to settle. The mother liquor was decanted away, and the remaining orange precipitate was extracted with 50 mL of benzene and filtered to afford a pale blue-green solution. Storage of the solution at *ca.* 7 °C for 12 h gave orange crystals of **6** (0.35 g, 40%). Mp (°C): 185−187 (dec). UV−vis (benzene) λ_{max} [nm] (ϵ in M^{-1} cm^{-1}): 598 (50). ^{1}H NMR (C_6D_6): δ 9.28 (s, 1H, $^1J_{Sn-H}$ = *ca.* 95 Hz, Sn-*H*), 7.30 (t, 2H, $^3J_{HH}$ = 7.5 Hz, Ar*H*), 7.03 (d, 4H, $^3J_{HH}$ = 7.5 Hz, Ar*H*), 6.82 (s, 2H, Ar*H*), 3.29 (s, 3H, OCH_3), 3.08 (septet, 4H, $^3J_{HH}$ = 6.9 Hz, C*H*(CH_3)$_2$), 1.04 (d, 12H, $^3J_{HH}$ = 6.6 Hz, CH(CH_3)$_2$), 0.95 (d, 12H, $^3J_{HH}$ = 6.9 Hz, CH(CH_3)$_2$). ^{119}Sn NMR (C_6D_6): δ 687 (br, $\Delta\omega_{1/2}$ = *ca.* 650 Hz). IR (Nujol, cm^{-1}): The Sn−H stretching band is likely obscured by ligand vibrations.

(4-^{t}Bu−Ar′)SnCl (9). A solution of [4-^{t}Bu−Ar′]Li (**8**) (4.00 g, 8.66 mmol) in 50 mL of diethyl ether was added dropwise to a slurry of $SnCl_2$ (1.93 g, 102 mmol) in 65 mL of cold (−78 °C) Et_2O. The resulting yellow slurry was slowly warmed to room temperature and stirred for 2 days. The solvent was then removed, and the product was extracted with 100 mL of warm toluene and filtered. Cooling of the pale orange filtrate to *ca.* −20 °C gave a crop of yellow microcrystalline **9** (2.39 g, 45%) after 1 week. Mp (°C): 216−218. UV−vis (hexanes) λ_{max} [nm] (ϵ in M^{-1} cm^{-1}): 402 (1240). ^{1}H NMR (C_6D_6): δ 7.38 (s, 2H, Ar*H*), 7.18−7.25 (m, 6H, Ar*H*), 3.12 (septet, 4H, $^3J_{HH}$ = 6.9 Hz, C*H*(CH_3)$_2$), 1.33 (d, 12H, $^3J_{HH}$ = 6.9 Hz, CH(CH_3)$_2$), 1.32 (s, 9H, C(CH_3)$_3$), 1.05 (d, 12H, $^3J_{HH}$ = 6.9 Hz, CH(CH_3)$_2$). ^{13}C{^{1}H} NMR (C_6D_6): δ 150.3, 147.7, 144.4, 129.3, 125.5, 123.7 and 122.8 (Ar*C*), 34.5 (*C*(CH$_3$)$_3$), 31.2 (*C*H(CH$_3$)$_2$), 30.9 (C(*C*H$_3$)$_3$), 26.1 (CH(*C*H$_3$)$_2$), 24.3 (CH(*C*H$_3$)$_2$), 22.8 (CH(*C*H$_3$)$_2$). ^{119}Sn NMR (C_6D_6): δ 1001 (br).

[(4-^{t}Bu−Ar′)Sn(μ-H)]$_2$ (10). To a mixture of **9** (0.64 g, 1.1 mmol) and $LiBH_4$ (0.031 g, 1.4 mmol) were added dropwise 20 mL of cold (*ca.* −20 °C) diethyl ether. The reaction was warmed to ambient temperature and stirred for 2 h to give a green solution over a white precipitate. The mixture was then filtered, and the solvent was removed to give a tan-orange solid (0.48 g, 80%). Crystals of suitable quality for X-ray diffraction (orange blocks) were grown from a benzene solution at *ca.* 7 °C. Mp (°C): darkens at 115, melts at 210. UV−vis (benzene) λ_{max} [nm] (ϵ in M^{-1} cm^{-1}): 594 (100). ^{1}H NMR (C_6D_6): δ 9.11 (s, 1H, $^1J_{Sn-H}$ = *ca.* 87 Hz, Sn-*H*), 7.38 (s, 2H, Ar*H*), 7.05−7.31 (m, 6H, Ar*H*), 3.07 (septet, 2H, $^3J_{HH}$ = 6.9 Hz, C*H*(CH_3)$_2$), 3.00 (septet, 2H, $^3J_{HH}$ = 6.6 Hz, C*H*(CH_3)$_2$), 1.32 (d, 6H, $^3J_{HH}$ = 6.6 Hz, CH(CH_3)$_2$), 1.32 (d, 6H, $^3J_{HH}$ = 6.6 Hz, CH(CH_3)$_2$), 1.24 (s, 9H, C(CH_3)$_3$), 1.03 (d, 6H, $^3J_{HH}$ = 6.9 Hz, CH(CH_3)$_2$), 0.92 (d, 6H, $^3J_{HH}$ = 6.9 Hz, CH(CH_3)$_2$). ^{13}C{^{1}H} NMR (C_6D_6): δ 147.3, 146.2, 140.9, 137.9, 129.6, 129.0, 127.4 and 123.9 (Ar*C*), 34.4 (*C*(CH$_3$)$_3$), 31.3 (*C*H(CH$_3$)$_2$), 31.0 (C(*C*H$_3$)$_3$), 30.8 (*C*H(CH$_3$)$_2$), 26.3 (CH(*C*H$_3$)$_2$), 24.4 (CH(*C*H$_3$)$_2$), 23.4 (CH(*C*H$_3$)$_2$), 22.8 (CH(*C*H$_3$)$_2$). ^{119}Sn{^{1}H} NMR (C_6D_6): δ 667 (br). IR (Nujol, cm^{-1}): The Sn−H stretching band is likely obscured by ligand vibrations.

(4-Me$_3$Si−Ar′)SnCl (13). A solution of (4-Me$_3$Si−Ar′)Li (**12**) (2.00 g, 4.30 mmol) in 40 mL of Et_2O was added dropwise to a precooled (−78 °C) suspension of $SnCl_2$ (1.20 g, 6.3 mmol) in 30 mL of Et_2O. The reaction mixture was allowed to slowly warm to room temperature and was stirred for a further 10 h, to give a bright orange reaction mixture. The volume of the reaction was concentrated to 10 mL, and 50 mL of hexanes were then added. The insoluble solids were separated by filtration and concentration of the filtrate to 30 mL, followed by cooling to *ca.* −20 °C affording **13** as an orange solid (1.65 g, 63%). Mp (°C): 154−155. UV−vis (hexanes) λ_{max} [nm] (ϵ in M^{-1} cm^{-1}): 406 (2400). ^{1}H NMR (C_6D_6): δ 7.54 (s, 2H, Ar*H*), 7.22 (t, 2H, $^3J_{HH}$ = 6.8 Hz, Ar*H*), 7.11 (d, 4H, $^3J_{HH}$ = 6.8 Hz, Ar*H*), 3.06 (septet, 4H, $^3J_{HH}$ = 6.9 Hz, C*H*(CH_3)$_2$), 1.27 (d, 12H, $^3J_{HH}$ = 6.9 Hz, CH(CH_3)$_2$), 1.00 (d, 12H, $^3J_{HH}$ = 6.9 Hz, CH(CH_3)$_2$), 0.24 (s, 9H, Si(CH_3)$_3$). ^{13}C{^{1}H} NMR (C_6D_6): δ 183.5, 148.3, 144.6, 140.0, 137.7, 135.9, 130.0 and 124.3 (Ar*C*), 31.6 (*C*H(CH$_3$)$_2$), 26.7 (CH(*C*H$_3$)$_2$), 23.4 (CH(*C*H$_3$)$_2$), −1.37 (Si(*C*H$_3$)$_3$). ^{29}Si NMR (C_6D_6): δ −4.3. ^{119}Sn{^{1}H} NMR (C_6D_6): δ 904.1.

[(4-Me$_3$Si−Ar′)Sn(μ-H)]$_2$ (14). To a mixture of $LiNMe_2$ (0.160 g, 3.11 mmol) and **13** (2.00 g, 3.11 mmol) were added 40 mL of cold (*ca.* −40 °C) diethyl ether. The resulting yellow slurry was warmed to ambient temperature and stirred overnight. The reaction mixture was then filtered through Celite to give a yellow filtrate which contained (4-Me$_3$Si−Ar′)SnNMe$_2$. A solution of BH_3·THF (3.40 mL, 1.0 M solution in THF, 3.40 mmol) was then added to the amide and yielded a deep green solution. The reaction was stirred for a further 45 min and then concentrated to *ca.* 10 mL, resulting in the precipitation of a tan colored solid. The mother liquor was decanted away from the insoluble precipitate (**14**), and the product was dried under vacuum (0.95 g, 50%). Crystals of **14** of suitable quality for X-ray diffraction (orange blocks) were subsequently obtained by cooling a solution of *in situ* generated **14** in diethyl ether (−20 °C). Mp (°C): darkens at 65, chars at 115 with gas evolution, melts at 160−161. UV−vis (benzene) λ_{max} [nm] (ϵ in M^{-1} cm^{-1}): 440 (shoulder), 582 (175). ^{1}H NMR (C_6D_6): δ 9.12 (s, 1H, $^1J_{Sn-H}$ = *ca.* 87 Hz, Sn-*H*), 7.33 (s, 2H, Ar*H*), 7.31 (m, 2H, Ar*H*), 7.04 (d, 4H, $^3J_{HH}$ = 7.5 Hz, Ar*H*), 3.01 (septet, 4H, $^3J_{HH}$ = 6.9 Hz, C*H*(CH_3)$_2$), 1.05 (d, 6H, $^3J_{HH}$ = 6.6 Hz, CH(CH_3)$_2$), 1.03 (d, 6H, $^3J_{HH}$ = 6.6 Hz, CH(CH_3)$_2$), 0.92 (d, 6H, $^3J_{HH}$ = 6.9 Hz, CH(CH_3)$_2$), 0.22 (s, 9H, Si(CH_3)$_3$). The insolubility of **14** precluded the acquisition of informative ^{13}C{^{1}H} and ^{119}Sn NMR spectra. IR (Nujol, cm^{-1}): The Sn−H stretching band is likely obscured by ligand vibrations.

(3,5-^{i}Pr$_2$−Ar*)SnCl (15). A solution of 3,5-^{i}Pr$_2$−Ar*Li(OEt$_2$)$_2$ (3.0 g, 4.2 mmol) in 40 mL of Et_2O was added dropwise to a precooled (−78 °C) mixture of $SnCl_2$ (1.18 g, 6.2 mmol) in 20 mL of diethyl ether. The reaction mixture quickly adopted a yellow-orange color that intensified upon warming to room temperature to produce a dark orange solution along with a white precipitate. The solvent was removed *in vacuo*, and the remaining residue was extracted with 80 mL of hexanes. The precipitated material (including excess $SnCl_2$) was removed by filtration, and the resulting deep-orange filtrate was concentrated to incipient crystallization. Cooling of the solution to *ca.* −20 °C yielded **15** (1.67 g, 56%) as orange crystals. Mp (°C): 149−151. UV−vis (hexanes) λ_{max} [nm] (ϵ in M^{-1} cm^{-1}): 416 (2700). ^{1}H NMR (C_6D_6): δ 7.47 (s, 1H, Ar*H*), 7.22 (s, 4H, Ar*H*), 2.98 (septet, 4H, $^3J_{HH}$ = 6.6 Hz, C*H*(CH_3)$_2$), 2.84 (septet, 2H, $^3J_{HH}$ = 6.6 Hz, C*H*(CH_3)$_2$), 2.75 (septet, 2H, $^3J_{HH}$ = 6.9 Hz, C*H*(CH_3)$_2$), 1.43 (d, 12H, $^3J_{HH}$ = 6.9 Hz, CH(CH_3)$_2$), 1.25 (d, 12H, $^3J_{HH}$ = 6.9 Hz, CH(CH_3)$_2$), 1.16 (d, 12H, $^3J_{HH}$ = 6.9 Hz, CH(CH_3)$_2$), 1.12 (d, 12H, $^3J_{HH}$ = 6.9 Hz, CH(CH_3)$_2$). ^{13}C{^{1}H} NMR (C_6D_6): δ 221.3, 149.9, 148.5, 148.1, 140.5, 134.0, 123.6 and 123.4 (Ar*C*), 35.0 (*C*H(CH$_3$)$_2$), 31.0 (*C*H(CH$_3$)$_2$), 30.1 (*C*H(CH$_3$)$_2$), 26.8 (CH(*C*H$_3$)$_2$), 25.7 (CH(*C*H$_3$)$_2$), 23.5 (CH(*C*H$_3$)$_2$). ^{119}Sn{^{1}H} NMR (C_6D_6): δ 961 (br).

(3,5-^{i}Pr$_2$−Ar*)SnSn(H)$_2$(3,5-^{i}Pr$_2$−Ar*) (16). A solution of DIBAL (0.26 g, 1.8 mmol) in 20 mL of Et_2O was added to an orange solution of **15** (1.27 g, 1.8 mmol) in 30 mL of Et_2O at −78 °C. Upon the addition

of DIBAL, a deep blue solution was observed. The reaction was allowed to warm to room temperature overnight, and the solvent was then removed under vacuum. The product was dissolved in 50 mL of hexanes and filtered, and the filtrate was concentrated to *ca.* 2 mL which yielded dark-blue crystals of **16** upon storage of the solution at *ca.* −20 °C for 2 weeks (0.90 g, 71%). Mp (°C): 153−154 (dec). UV−vis (hexanes) λ_{max} [nm] (ϵ in M^{-1} cm^{-1}): 422 (540), 480 (shoulder), 622 (220). ^{1}H NMR (C_6D_6): δ 7.92 (s, 2H, $^1J_{Sn-H}$ = *ca.* 528 Hz, Sn-*H*), 7.43 (s, 2H, Ar*H*), 7.11 (s, 8H, Ar*H*), 2.93 (overlapping septets, 12H, C*H*(CH_3)$_2$), 2.54 (septet, 4H, $^3J_{HH}$ = 6.6 Hz, C*H*(CH_3)$_2$), 1.36 (d, 48H, $^3J_{HH}$ = 6.9 Hz, CH(C*H*$_3$)$_2$), 1.19 (d, 48H, $^3J_{HH}$ = 6.9 Hz, CH(C*H*$_3$)$_2$). ^{13}C{^{1}H} NMR (C_6D_6): δ 148.2, 147.8, 147.7, 142.4, 136.4, 124.0 and 122.7 (Ar*C*), 34.4 (*C*H(CH_3)$_2$), 30.9 (*C*H(CH_3)$_2$), 30.1 (*C*H(CH_3)$_2$), 27.6 (CH(*C*H$_3$)$_2$), 26.1 (CH(*C*H$_3$)$_2$), 25.9 (CH(*C*H$_3$)$_2$), 24.6 (CH(*C*H$_3$)$_2$) (ipso carbon not observed). ^{119}Sn{^{1}H} NMR (C_6D_7, 25 °C): δ 1727. ^{119}Sn{^{1}H} NMR (C_6D_7, −70 °C): δ 34. IR (Nujol, cm^{-1}): 1810 (m) and 1783 (m) [Sn−H stretches]. ^{119}Sn Mössbauer (90 K, mm s^{-1}): Site A: IS = 1.370(4) [QS = 0.967(4)]; Site B: IS = 3.252(7) [QS = 3.713(7)].

Results and Discussion

Synthesis and Spectroscopy of the Terphenyl Tin(II) Hydrides [Ar*Sn(μ-H)]$_2$ (Ar* = C$_6$H$_3$-2,6-(C$_6$H$_2$-2,4,6-^{i}Pr$_3$)$_2$) and [Ar′Sn(μ-H)]$_2$ (Ar′ = C$_6$H$_3$-2,6-(C$_6$H$_3$-2,6-^{i}Pr$_2$)$_2$). The first stable tin(II) hydride [Ar*Sn(μ-H)]$_2$ (**17**) was synthesized in 2000 via reduction of the corresponding chloride [Ar*Sn(μ-Cl)]$_2$ with DIBAL.[6] Stability was conferred by use of the sterically crowding terphenyl ligand Ar* (Ar* = C$_6$H$_3$-2,6-(C$_6$H$_2$-2,4,6-^{i}Pr$_3$)$_2$). It was isolated as orange crystals that dissolved in hydrocarbons to produce an intense blue solution. The color change was originally interpreted in terms of its dissociation into Ar*SnH monomers which had a blue color as a result of an n−p transition. ^{1}H NMR spectroscopy afforded a signal at 7.87 ppm attributable to the Sn−H moiety that displayed a $^1J_{Sn-H}$ of 592 Hz. We decided to build upon these studies by employing the slightly less hindered Ar′ ligand (Ar′ = C$_6$H$_3$-2,6-(C$_6$H$_3$-2,6-^{i}Pr$_2$)$_2$) with the object of isolating higher oligomers (i.e., trimers) in the solid state.

The corresponding reduction of [Ar′Sn(μ-Cl)]$_2$ with DIBAL was explored as a method to prepare Ar′SnH; however this route did not yield clean products. Noting that diborane was used previously to generate organotin(IV) hydrides, R$_3$SnH, from organotin(IV) amide precursors,[27] we decided first to prepare the aryltin amide, Ar′SnNMe$_2$ (**1**), and then explore its reactivity toward BH$_3$·THF to obtain the desired tin(II) hydride. Upon treating a bright yellow solution of **1** in Et$_2$O with a slight excess of BH$_3$·THF, a deep-blue solution was immediately seen which later (*ca.* 30 min) became pale green as copious amounts of a microcrystalline orange solid precipitated. This orange solid was later identified as the dimeric hydride species [Ar′Sn(μ-H)]$_2$ (**2**) by X-ray crystallography.[13] In contrast to **17**, the less-hindered **2** was only sparingly soluble in typical organic solvents (hexanes, THF, ether, and benzene) and showed a tendency to decompose over time in solution. Dissolution of this product in C_6D_6 afforded a pale-blue solution, and examination of the ^{1}H NMR spectrum revealed the presence of a number of ligand-based resonances along with a significantly deshielded signal at 9.13 ppm. The latter resonance contained two broad flanking satellites in the correct intensity for coupling of a proton to $^{117/119}$Sn nuclei (I = $^1/_2$; abundance = *ca.* 8% each). From this feature we were able to extract an averaged $^1J_{Sn-H}$ coupling constant of 89 Hz, which was considerably smaller than the Sn−H coupling (592 Hz) observed for **17** in solution.[6] For comparison, typical values of $^1J_{Sn-H}$ for organotin(IV) hydrides are much larger and are typically near ∼1900 Hz.[28] Presumably, the weaker Sn−H bonds in the bridged structure account for the unusually low value of the $^1J_{Sn-H}$ coupling. The spectral data for **2** are therefore consistent with the retention of a bridged structure in solution while it appears that **17** adopts a different structure from **2** in solution (see below). The IR spectra of **2** and **17** also display major differences. In contrast to **17** which features two well-defined, moderately intense Sn−H stretching vibrations at 1828 and 1771 cm^{-1} in the IR spectrum, the less-hindered hydride, **2**, displayed no IR bands in the region 1500 to 2800 cm^{-1}.[29]

Chart 2. Terphenyl Ligands Used to Construct the Aryltin(II) Hydrides

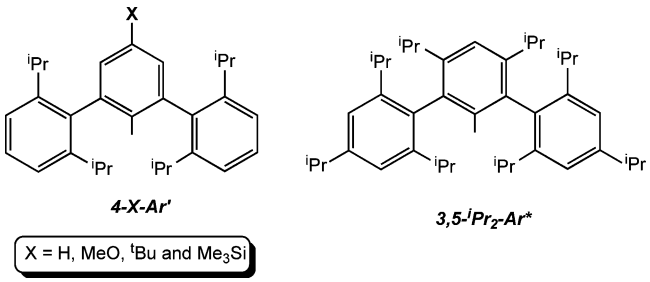

In summary the experimental data for [Ar*Sn(μ-H)]$_2$ and [Ar′Sn(μ-H)]$_2$ show that, although their solid-state structures are similar, their solution behavior differs markedly as a result of the para substituents on the flanking aryl rings. However the identity of the species present in solutions of **17** was only established by further variation of the electronic and steric properties of the terphenyl ligands discussed below.

Use of Electronically and Sterically Modified Terphenyl Ligands. We prepared an analogous series of Sn(II) hydrides with the use of modified terphenyl ligand derivatives designated 4-X−Ar′ and 3,5-^{i}Pr$_2$−Ar* (Chart 2) to investigate the effects of the substituents on the hydride structure.

Beginning with the readily synthesized precursor, 4-MeO−Ar′Li, featuring an electron-withdrawing methoxy group, we were able to prepare the requisite tin(II) chloride [(4-MeO−Ar′)Sn(μ-Cl)]$_2$ (**5**) by reaction with anhydrous SnCl$_2$ in diethyl ether. Compound **5** was obtained as a highly crystalline orange solid and was shown by X-ray crystallography to possess a dimeric structure held together by Sn−Cl bridging interactions.[30] Conversion of **5** into the tin(II) hydride, [4-MeO−Ar′)Sn(μ-H)]$_2$ (**6**), was possible using DIBAL; however we obtained significantly purer material when LiBH$_4$ was used as the reducing agent (Scheme 1). A terphenyltin(II) hydride containing an electron-releasing *tert*-butyl group in the 4-position of the central aryl ring was also prepared. The precursor terphenyliodide, 4-^{t}Bu−Ar′I (**7**) was synthesized in a multistep procedure (see Supporting Information for details) and converted into [(4-

(27) (a) Kula, M.-R.; Lorberth, J.; Amberger, E. *Chem. Ber.* **1964**, *97*, 2087. (b) For a similar transformation using silanes, see: Hays, D. S.; Fu, G. C. *J. Org. Chem.* **1997**, *62*, 7070.

(28) (a) Gil, V. M. S.; Philipsborn, W. v. *Magn. Reson. Chem.* **1989**, *27*, 409. (b) Curran, D. P.; Hadida, S.; Kim, S.-Y.; Luo, Z. *J. Am. Chem. Soc.* **1999**, *121*, 6607.

(29) (a) Harrison, P. G. *Chemistry of Tin*; Chapman and Hall: New York, 1989. (b) Saito, M.; Hashimoto, H.; Tajima, T.; Ikeda, M. *J. Organomet. Chem.* **2007**, *692*, 2729.

(30) The structures of the substituted (4-X-Ar′)SnCl derivatives will be discussed in a forthcoming publication.

Scheme 1. Preparative Routes to Terphenyl Tin(II) Hydrides

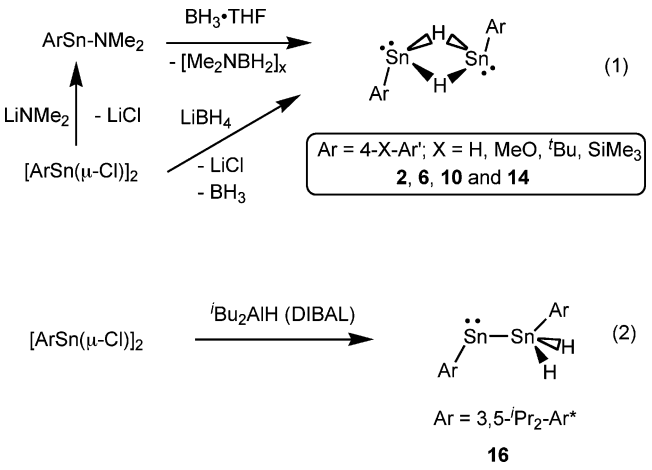

^{t}Bu−Ar′)Sn(μ-H)]$_2$ (**10**) according to Scheme 1 (via $LiBH_4$). As with **2**, compounds **6** and **10** were obtained as orange crystals that were only sparingly soluble in organic solvents. Well-separated singlet resonances were observed at 9.28 and 9.11 ppm in the ^{1}H NMR spectra (C_6D_6) of **6** and **10**. Each signal had broad tin satellites from which an average $^1J_{Sn-H}$ coupling constant of *ca.* 90−95 Hz could be obtained. Furthermore compounds **2**, **6**, and **10** each gave similar UV−vis spectra with weak absorptions positioned at 595, 598, and 594 nm, respectively. Attachment of a lipophilic ^{t}Bu group onto the Ar′ ligand in **10** made the hydride sufficiently soluble in C_6D_6 to quickly record ^{13}C{^{1}H} and ^{119}Sn NMR spectra. Consequently a broad resonance located at 667 ppm was observed in the ^{119}Sn NMR spectrum of **10**; however the width of this signal (*ca.* 450 Hz) was too large to allow for the determination of the Sn−H coupling constant in the proton-coupled ^{119}Sn NMR spectrum. Using significantly longer acquisition times (up to 24 h) the ^{119}Sn NMR spectra of **2** and **6** were also recorded and gave similarly broad resonances at 657 and 687 ppm, respectively. These results showed that compounds **2**, **6**, and **10** all have similar structures in solution. Each of the tin(II) hydrides showed signs of decomposition (charring) upon heating to *ca.* 100 °C in the solid state; however samples of these hydrides decompose in solution over time at much lower temperatures (40 °C) to yield unknown species that we are currently trying to identify.

A further hydride [(4-Me$_3$Si−Ar′)Sn(μ-H)]$_2$ (**14**), containing a *para*-trimethylsilyl group as part of the terphenyl ligand, was prepared because of an unusual prior result in which the distannyne (4-Me$_3$Si−Ar′)SnSn(4-Me$_3$Si−Ar′) (**18**) was found to have a strongly bent structure and a long Sn−Sn bond in comparison to the correspondingly wide C−Sn−Sn angle and multiple Sn−Sn bonding in the Ar′SnSnAr′ analogue.[31] To investigate this phenomenon further, and to rule out the possibility that **18** was actually a tin(II) hydride,[32] **14** was synthesized using a similar amide metathesis route as that employed for **2**. Specifically, treatment of *in situ* generated tin(II) amide, (4-Me$_3$Si−Ar′)SnNMe$_2$, with a slight excess of BH_3•THF gave the hydride [(4-Me$_3$Si−Ar′)Sn(μ-H)]$_2$ (**14**) as orange crystals. This compound, once crystallized, was almost insoluble in benzene which precluded the observation of solution ^{13}C-{^{1}H} and ^{119}Sn NMR data. However the ^{1}H NMR spectrum of **14** in C_6D_6 yielded a characteristic singlet at 9.12 ppm, which was flanked by diagnostic Sn−H satellites ($^1J_{Sn-H}$ = *ca.* 87 Hz), suggesting that this species was structurally similar to the other [(4-X−Ar′)Sn(μ-H)]$_2$ derivatives discussed above. Notably, the ligand ^{1}H NMR signals and UV−vis spectrum of **14** differed substantially from those reported for the dark green distannyne **18**. Moreover, while the distannyne melts without decomposition at 181 °C, the hydride analogue **14** shows marked signs of decomposition at 65 °C with eventual melting occurring at 160 °C. These observations, along with the results from X-ray crystallography (see below), eliminate the possibility that the previously reported species **18** was the hydride bridged product [(4-Me$_3$Si−Ar′)Sn(μ-H)]$_2$.

In addition to the above ligands, we decided to investigate the use of the extremely hindered terphenyl ligand 3,5-^{i}Pr$_2$−Ar* (3,5-^{i}Pr$_2$−Ar* = 3,5-^{i}Pr$_2$−C$_6$H-2,6-(C$_6$H$_2$-2,4,6-^{i}Pr$_3$)$_2$; Chart 2) which had already been shown to yield species whose structures differ considerably from those with the less bulky Ar′ ligand. For example, the unusual chromium(I) complex [(3,5-^{i}Pr$_2$−Ar*)Cr•THF][33] was isolated and can be formally regarded as a base-stabilized monomer surrogate of the known multiply bonded chromium(I) dimer Ar′CrCrAr′.[34] In a similar manner as that reported for the synthesis of **17**, the reaction of (3,5-^{i}Pr$_2$−Ar*)SnCl (**15**) with DIBAL gave a deep-blue solution from which small, dark-blue, platelike crystals were obtained and identified as the asymmetric tin(II) hydride (3,5-^{i}Pr$_2$−Ar*)-SnSn(H)$_2$(3,5-^{i}Pr$_2$−Ar*) (**16**).

It is noteworthy that both **16** and **17** have similar deep blue colors in solution, suggesting that these species have similar structures when dissolved. The UV−vis spectrum of **16** in hexanes consists of three relatively weak absorptions at 422, 480, and 622 nm, respectively, while **17** displays a single broad absorption at 608 nm of moderate intensity (ϵ = 160 M^{-1} cm^{-1}). The IR spectrum of **16** revealed two sharp bands of medium intensity located at 1810 and 1783 cm^{-1} which are close to the range of 1900 ± 50 cm^{-1} observed for Sn(IV) hydrides.[29] This is consistent with the retention of an asymmetric mixed-valent structure for **16** in solution. Significantly, very similar Sn−H stretches were also observed in the IR spectrum of **17** [1828 and 1771 cm^{-1}, respectively], and a color change from orange to blue was noted upon sample dissolution.[6] Thus, it seems likely that the centrosymmetric structure of **17** found in the solid state is mostly converted into the mixed-valent form Ar*SnSn(H)$_2$Ar* and not the originally proposed monomer Ar*SnH, upon dissolution in Nujol.

The ^{1}H NMR spectrum of **16** in deuterated toluene at room temperature showed only one set of signals for the aryl ligands. In addition, a broad singlet at 7.92 ppm was present and was assigned as a tin hydride resonance because of the observation of accompanying tin satellites (average $^1J_{Sn-H}$ = *ca.* 528 Hz). For comparison, the hydride resonance in **17** (7.87 ppm) is very similar with a Sn−H coupling constant of 592 Hz.[6] The ^{1}H

(31) Fischer, R. C.; Pu, L.; Fettinger, J. C.; Brynda, M. A.; Power, P. P. *J. Am. Chem. Soc.* **2006**, *128*, 11366.
(32) It is often difficult to discount the presence of hydrogen atoms using X-ray crystallography alone; see: (a) Schneider, J. J.; Goddard, R.; Werner, S.; Krüger, C. *Angew. Chem., Int. Ed. Engl.* **1991**, *30*, 1124. (b) Abrahamson, A. B.; Niccolai, G. P.; Heinekey, D. M.; Casey, C. P.; Bursten, B. E. *Angew. Chem., Int. Ed. Engl.* **1992**, *31*, 471. (c) Kersten, J. L.; Rheingold, A. L.; Theopold, K. H.; Casey, C. P.; Widenhoefer, R. A.; Hop, C. E. C. A. *Angew. Chem., Int. Ed. Engl.* **1992**, *31*, 1341. (d) Lutz, F.; Bau, R.; Wu, P.; Koetzle, T. F.; Krüger, C.; Schneider, J. J. *Inorg. Chem.* **1996**, *35*, 2698.
(33) Wolf, R.; Brynda, M.; Ni, C.; Long, G. J.; Power, P. P. *J. Am. Chem. Soc.* **2007**, *129*, 6076.
(34) Nguyen, T.; Sutton, A. D.; Brynda, M.; Fettinger, J. C.; Long, G. J.; Power, P. P. *Science* **2005**, *310*, 844.

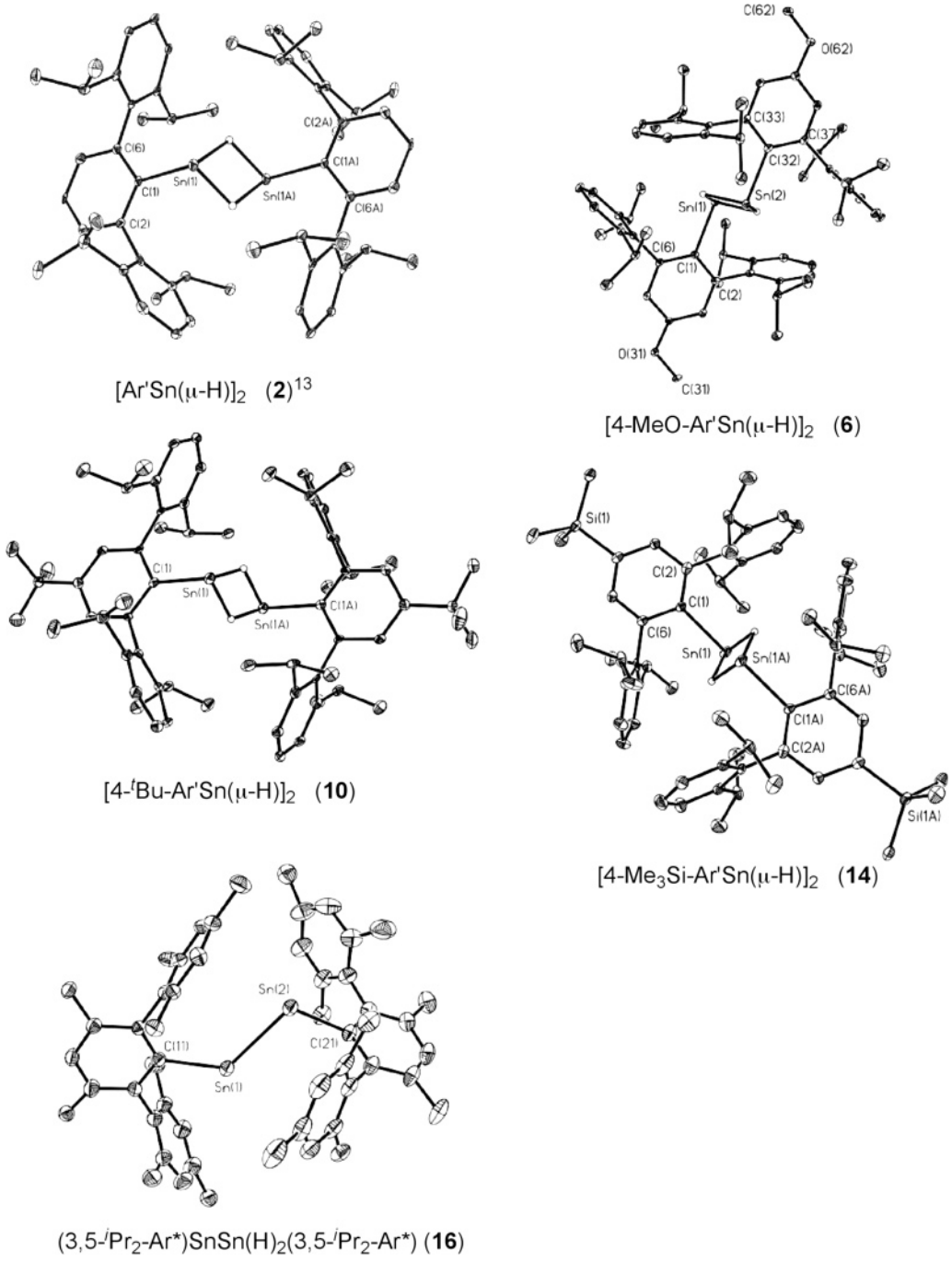

Figure 1. Molecular structures of tin hydrides **2**, **6**, **10**, **14**, and **16** at the 30% probability level with carbon-bound hydrogen atoms removed for clarity. For **16** the Me groups of the ^{i}Pr moieties have also been removed for clarity.

NMR spectrum of **16** shows dynamic behavior and the Sn−H resonances become sharper as the temperature is lowered. Furthermore at −70 °C, the signals for the 3,5-^{i}Pr$_2$−Ar* ligands become more numbered, indicating a lowering of symmetry that is possibly due to restricted rotation of the terphenyl ligands. Despite the apparent lowering in symmetry, only a single Sn−H environment could be found as evidenced by a shifted resonance at 7.42 ppm which displayed well-resolved Sn−H coupling [$^{1}J_{119\mathrm{Sn-H}} = 1288$ Hz; $^{1}J_{117\mathrm{Sn-H}} = 1234$ Hz). These values are more than twice as large as those observed for **17** (and **16** at room temperature), although they are smaller than typical Sn−H coupling constants found in tetravalent tin(IV) hydrides (*ca.* 1900 Hz).[28] A possible explanation for these observations will be detailed below.

X-ray Crystal Structures of the Tin(II) Hydrides. The structures of the terphenyltin(II) hydrides are found in Figure 1. The 4-X−Ar′ substituted tin hydrides **2**, **6**, **10**, and **14** adopt centrosymmetric structures with highly pyramidalized Sn coordination and planar Sn_2H_2 cores; a similar structural arrangement was also observed for the more hindered Ar* derivative **17**.[6] In addition, the terphenyl ligands occupy relative positions that are trans to each other, thus minimizing interligand repulsion. The Sn−Sn separations in **2**, **6**, and **10** (Table 2) were in the narrow range 3.1150(10) to 3.1260(11) Å, while the

Table 2. Selected Bond Lengths (Å) and Angles (deg) for the Reported Tin(II) Hydrides with Standard Deviations in Parentheses

compound	**2**	**6**	**10**	**14**	**16**
Sn−Sn	3.1260(11)	3.1176(4)	3.1150(10)	3.0532(8)	2.9157(10)
Sn−C(ipso)	2.221(6)	2.216(4)	2.208(6)	2.216(3)	2.228(5)
		2.219(4)		2.200(3)	2.247(6)
Sn−H	1.82(8)	1.94(2)	1.93(2)	1.95(3)	
	1.99(8)	1.94(2)		1.90(3)	
C(ipso)−Sn−Sn	98.11(5)	94.32(9)	95.29(14)	96.18(7)	126.44(15)
		95.18(10)		101.3(7)	106.37(17)
C(ipso)−Sn−H	99(2)	91(2)	100.0(19)	95.1(11)	
		91.9(15)		98.5(11)	

silylated derivative **14** had a Sn−Sn distance that was *ca.* 0.06 Å shorter [3.0532(8) Å]. For comparison the Ar* derivative **17** had a Sn−Sn distance of 3.1192(3) Å. The average bridging Sn−H distances in each of the dimers are 1.91−1.94(2) Å and are significantly longer than the terminal Sn−H bond [1.74(3) Å] in the monomeric species [{HC(CMeNDipp)$_2$}SnH] reported by Roesky et al.[7] It is interesting to note that the presence of bridging hydrides in **2** leads to a dramatic change in the overall structure when compared to the hydride-free distannyne analogue Ar′SnSnAr′ (**19**).[35] For example, the deep green distannyne **19** has a much wider C(ipso)−Sn−Sn angle [126.24(7)°] and a Sn−Sn distance [2.6675(4) Å] that is *ca.* 0.5 Å shorter than that in **2**. In addition, the relative orientation of the central aryl rings of the terphenyl ligands are coplanar with the C−Sn−Sn−C unit in **19**, while in **2** these rings are canted to an approximately orthogonal arrangement. The preparation and structural characterization of the hydride analogue **2** is valuable in reinforcing our initial assignment of the structure Ar′SnSnAr′, as it is often difficult to rule out the presence of hydrogen atoms bound to heavy atoms by X-ray crystallography alone.[32]

For reasons stated above, we also obtained the X-ray structure of the silylated derivative **14**. The overall structure of hydride [(4-Me$_3$Si−Ar′)Sn(μ-H)]$_2$ (**14**) is similar to that of the distannyne (4-Me$_3$Si−Ar′)SnSn(4-Me$_3$Si−Ar′) (**18**).[31] However in the case of **18** we were not able to observe any hydrogen atoms bound to tin. We have subsequently repeated the synthesis of **18** by the reduction of the tin(II) chloride **13** with potassium metal and have obtained an extremely high quality structure of **18** (*R* value <2.5%). As before, the overall structure of **18** was similar to that of **14**, and we could not locate any tin-bound hydrogen atoms (however all of the ligand bound hydrogen atoms could be located). The Sn−Sn distance in **18** [3.0660(10) Å; C(ipso)−Sn−Sn angle: 99.25(14)°][31] is close to the value found in **14**; however it is still different within experimental error. It is important to mention that crystals of **14** and **18** have vastly different physical and spectroscopic properties (*vide supra*). These observations show that compounds **14** and **18** are indeed distinct species but that their similar geometries are likely due to packing effects that are largely controlled by the bulky 4-Me$_3$-Si−Ar′ ligands.

The structure of the most hindered tin(II) hydride analogue **16** differed greatly from those of compounds **2**, **6**, **10**, and **14** (Figure 1). The most striking feature of the dinuclear complex **16** is the significantly shorter Sn−Sn distance [2.9157(10) Å] which is 0.15−0.2 Å shorter than that in any of the other tin(II) hydrides. This Sn−Sn distance is indicative of a lengthened single bond as typical Sn−Sn single bonds within distannanes R$_3$SnSnR$_3$ are in the range 2.76 to 2.88 Å.[36] The terphenyl ligands in **16** display two different orientations, with one of the two central aryl rings being twisted nearly perpendicular to the C(ipso)−Sn−Sn−C(ipso) unit [C(22)−C(21)−Sn(2)−Sn(1) dihedral angle: −76.8°], whereas the other is arranged in a coplanar fashion. Two different C(ipso)−Sn−Sn angles [126.44(15)° and 106.37(17)°] are observed which are much wider than the Sn−Sn−C(ipso) angles in the corresponding centrosymmetric terphenyltin(II) hydrides where these angles are in the range: 94.32(9)° to 101.03(7)°. Unfortunately the tin-bound hydrogen atoms in **16** could not be located by X-ray crystallography due to the modest quality of the data. However the different C(ipso)−Sn−Sn angles, the twisting of the aryl ligands, and the short Sn−Sn distance strongly support the presence of a mixed-valent tin(I/III) hydride in which two hydrogen atoms are bound to Sn(1) (corresponding to form **II** in Chart 1). The assignment of the Sn−H groups to Sn(1) is also supported by the structures of the mixed-valent species Ar*SnSn(R)$_2$Ar* (R = Me and Ph; **20** and **21**) which have C(ipso)−Sn−Sn angles of 119.30(6)° and 101.17(5)° for **20** and 113.01(6)° and 108.46(8)° for the phenylated analogue **21**; of note, both **20** and **21** have wider intraligand angles at tin when R groups are bound.[37,38] Moreover, compounds **20** and **21** have similar Sn−Sn bond lengths [2.8909(2) and 2.9688(2) Å, respectively] to that in **16** [2.9157(10) Å], consistent with a similar bonding environment within each of these mixed valent species.

Table 3. Selected Mössbauer Parameters (in mm s^{-1}) at 90 K for Compounds **2**, **16**, and **20**

parameter	**2** [Ar′Sn(μ-H)]$_2$	**16** (3,5-^{i}Pr$_2$–Ar*)SnSn(H)$_2$ (3,5-^{i}Pr$_2$–Ar*)	**20** Ar*SnSnMe$_2$Ar*
isomer shift (IS)	2.805(4) orange[a]	1.370(4) [site A]	1.29(1)
	2.800(3) green[a]	3.252(7) [site B]	2.70(1)
			3.00(1) [site C][b]
quadrupolar splitting (QS)	2.992(4) orange	0.967(4) [site A]	0.32(1)
	2.997(5) green	3.713(7) [site B]	4.50(1)
			2.05(1) [site C][b]

[a] Compound **2** exhibits photochromism (see Experimental Section for details). [b] For compound **20** site C has been assigned to monomeric Ar*SnMe. The three Mössbauer environments in **20** have essentially equal absorption areas.

Mössbauer Spectroscopy of Compounds 2 and 16. To further establish the mixed-valent structure of **16** beyond any doubt, Mössbauer data were recorded. For comparison, a spectrum of the symmetric tin(II) hydride **2** was also obtained (Table 3). The Mössbauer spectrum of **2** (Figure 2) is in agreement with the X-ray data and reveals the presence of a single tin(II) environment, with a doublet at 2.805(4) mm s^{-1}. The quadrupolar splitting (QS) associated with **2** was quite large [2.992(4) mm s^{-1}] and indicates a highly asymmetric electronic environment is present at the tin center. In the case of **16**, a more complicated spectrum was obtained which contained two distinct tin sites in an approximately equal intensity ratio. The first tin resonance [site A; IS = 1.370(4) mm s^{-1}] corresponds

(35) (a) Phillips, A. D.; Wright, R. J.; Olmstead, M. M.; Power, P. P. *J. Am. Chem. Soc.* **2002**, *124*, 5930. (b) Power, P. P. *Chem. Commun.* **2003**, 2091.
(36) (a) Párkányi, L.; Kálmán, A.; Pannell, K. H.; Cervantes-Lee, F.; Kapoor, R. N. *Inorg. Chem.* **1996**, *35*, 6622. (b) Puff, H.; Breuer, B.; Gehrke-Brinkmann, Kind, P.; Reuter, H.; Schuh, W.; Wald, W.; Weidenbrück, G. *J. Organomet. Chem.* **1989**, *363*, 265. (c) Kleiner, N.; Dräger, M. *J. Organomet. Chem.* **1984**, *270*, 151.
(37) Eichler, B. E.; Power, P. P. *Inorg. Chem.* **2000**, *39*, 5444.
(38) Phillips, A. D.; Hino, S.; Power, P. P. *J. Am. Chem. Soc.* **2003**, *125*, 7520.

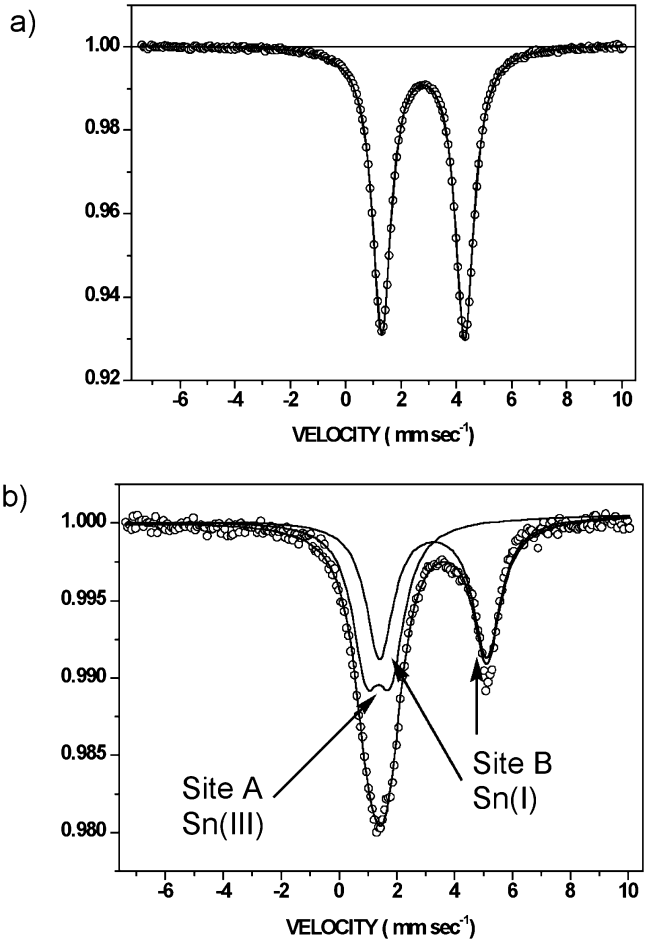

Figure 2. Mössbauer spectra for $[Ar'Sn(\mu\text{-}H)]_2$ (**2**) (a) and (3,5-^{i}Pr$_2$−Ar*)-SnSn(H)$_2$(3,5-^{i}Pr$_2$−Ar*) (**16**) (b).

to the tetravalent, formally Sn(III) site in **16**, while the remaining resonance at IS = 3.252(7) mm s^{-1} is assigned to the lower oxidation state, divalent Sn(I) center (site B). Both of the resonances for **16** were split into doublets with the more asymmetrically coordinated divalent Sn(I) site B having a larger quadrupolar splitting [3.713(7)] than the tetravalent site A which likely contains two bound hydrogen atoms [QS of site A = 0.967(4) mm s^{-1}]. The temperature dependence of the recoil-free fraction over the range $92 \leq T \leq 170$ K is identical for the two sites within experimental error. These data are consistent with our prior assignment of an asymmetric structure for **16** with two hydrogen atoms located on a single tin site. Interestingly, the Mössbauer spectrum of the related species Ar*SnSnMe$_2$-Ar* **20** has quite similar parameters (Table 3).[39]

Solid-State Structures and Theoretical Analysis. Although the calculations of Trinquier on the isomers **I**−**IV** of Sn_2H_4 showed that they do not differ greatly in energy,[8,40] the large size discrepancy between hydrogen and the terphenyl ligands made detailed calculations on the relative stabilities of forms **I**, **II**, and **IV** in the tin(II) hydride analogues $(ArSnH)_2$ featuring the same ligand series as employed in our experimental studies (namely Ar′, Ar*, and 3,5-^{i}Pr$_2$−Ar*) desirable.

Figure 3 shows the results of calculations on the least hindered member of the terphenyltin(II) hydride series, $(Ar'SnH)_2$. It is noteworthy that each of the calculated structures are close in energy (within 7 kcal mol^{-1}). When the Ar′ ligand is present, the most stable gas-phase structure is actually the asymmetric form related to **II**, while the formally double-bonded isomer **I** is only less stable by 2.2 kcal mol^{-1}. Interestingly, the hydride-bridged form **IV** is the least stable isomer by 7.0 kcal mol^{-1}. Nonetheless, this is the form that $(Ar'SnH)_2$ adopts in the solid state. From these data it is anticipated that, due to the low energy difference between each of the isomers, factors such as crystal packing forces could become very important in dictating which structure is favored upon crystallization. For example the known, multiply bonded, trans-bent stannyne Ar′SnSnAr′ (**19**) was calculated to be only 5.3 kcal mol^{-1} more stable than the more strongly bent, formally singly bonded isomer shown at the top right of Figure 3.[41,42] However by adding a remote trimethylsilyl group at the 4-position of the central ring of the terphenyl ligand, we have been able to crystallize a single-bonded form in the solid state, (4-Me$_3$Si−Ar′)SnSn(4-Me$_3$Si−Ar′) (**18**),[31] that has overall metrical parameters which match closely those listed in Figure 3. The calculated structure for the hydride-bridged isomer $[Ar'Sn(\mu\text{-}H)]_2$ corresponds reasonably well to the structure of **2** determined by X-ray crystallography. The calculated Sn−Sn separation (3.191 Å) is *ca.* 0.06 Å longer than that in **2** [3.1260-(11) Å] while the C(ipso)−Sn−Sn angle was nearly identical [98.0° vs 98.11(15)° in **2**]. Furthermore, the structure of **2** contains central terphenyl rings that are oriented orthogonally to the Sn_2H_2 core, which is also reproduced by the theoretical data (see Supporting Information for more details).

Various isomers of $(Ar*SnH)_2$ were calculated and shown to have relative energies within *ca.* 7 kcal mol^{-1} of each other (Figure 4). The hydride-bridged form $[Ar*Sn(\mu\text{-}H)]_2$ was calculated to be the least stable entity, and the asymmetric form, Ar*SnSn(H)$_2$Ar*, the most stable. However, as in the case of the Ar′ derivative, the hydride-bridged isomer is the form obtained upon crystallization of $(Ar*SnH)_2$. In other words crystallization does not yield the most stable structures calculated for the gas phase.

When the relative energies of the possible isomers of the bulky tin(II) hydride $[(3,5\text{-}^i Pr_2\text{−}Ar*)SnH]_2$ were calculated (Figure 4), the most stable isomer was also predicted to be the asymmetric form **II**. However the presence of the added ^{i}Pr$_2$ ligands in 3,5-^{i}Pr$_2$−Ar* destabilizes both the Sn−Sn bonded form **I** and the hydride-bridge structure **IV** to the extent that the latter isomer now lies higher in energy (relative to the asymmetric form **II**) by 14.3 kcal mol^{-1}. Apparently the added bulk within the 3,5-^{i}Pr$_2$−Ar* ligand has a significant effect on the relative stability of the various tin(II) hydride forms in the gas phase, and contrary to what was observed with the Ar′ and Ar* ligands, the energy difference is sufficiently large to ensure that the asymmetric form is the one that is obtained on crystallization (cf. structure of **16**). The calculated structure of **16** reproduces well the experimentally determined Sn−Sn and Sn−C bond lengths [Sn−Sn: 2.959 Å vs 2.9157(10) Å in **16**; Sn−C(ipso): 2.230 and 2.248 Å vs 2.228(5) and 2.247(6) Å in **16**]. However each of the calculated Sn−Sn−C(ipso) angles is overestimated by 6°−18° [111.9° and 144.7° vs 106.37(17)°

(39) Power, P. P.; Stanciu, C.; Nowik, I.; Herber, R. H. *Inorg. Chem.* **2005**, *44*, 9461.
(40) Our calculations show that the asymmetric species HSn−SnH$_3$ (form **II**) is the most stable isomer of the Sn_2H_4 isomer series. This is in contrast to work by Trinquier (ref 8) which showed that the hydride-bridged isomer $[HSn(\mu\text{-}H)]_2$ was the most stable form. These differences are likely a reflection of the higher level of calculations used in this present study.
(41) Takagi, N.; Nagase, S. *Organometallics* **2007**, *26*, 469.
(42) Takagi, N.; Nagase, S. *Organometallics* **2007**, *26*, 3627.

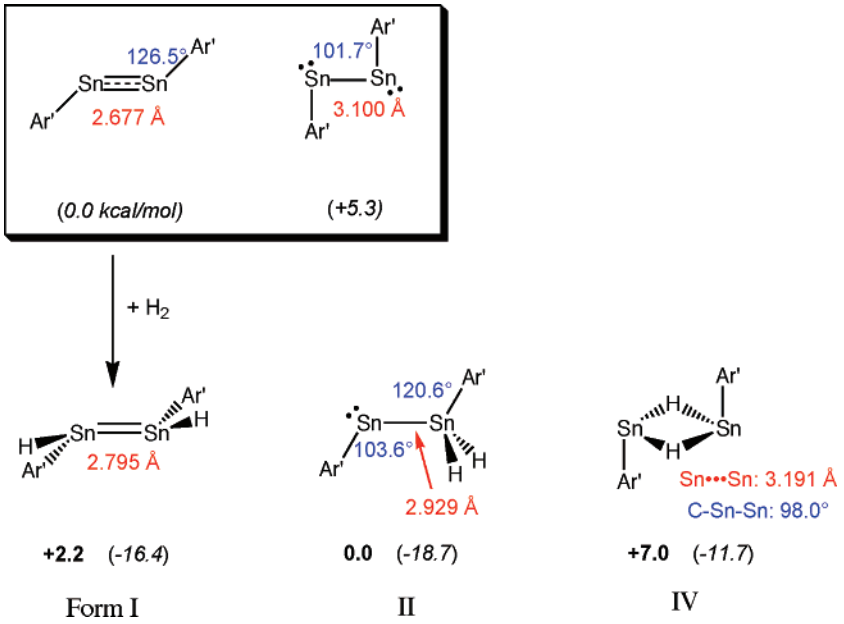

Figure 3. Calculated energies and selected geometric parameters for various isomer forms of $(Ar'SnH)_2$ at the B3PW91 level. Values in parentheses correspond to energies relative to Ar′SnSnAr′ (set at 0.0 kcal/mol).

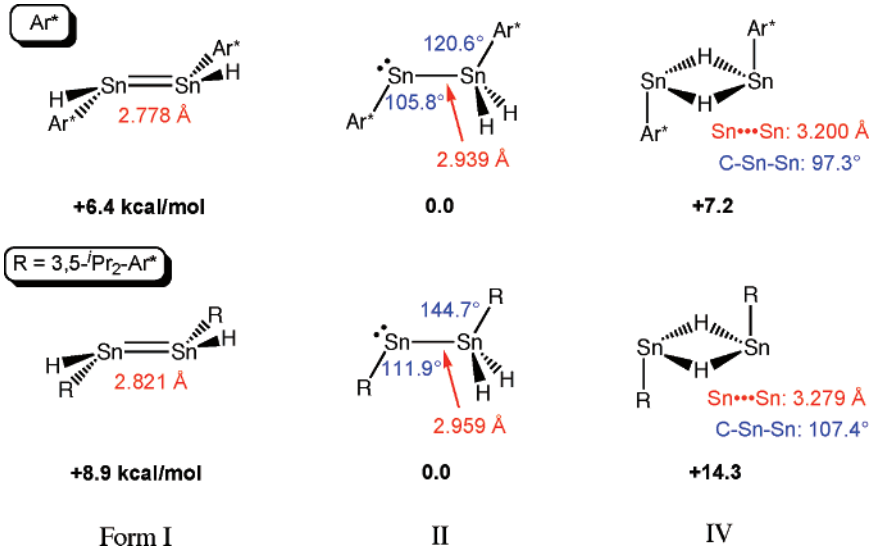

Figure 4. Calculated relative energies and selected geometric parameters for various isomer forms of $(Ar*SnH)_2$ and $[(3,5\text{-}^iPr_2\text{−}Ar*)SnH]_2$ at the B3PW91 level.

and 126.44(15)°]. The location of two hydrogen atoms at the tin center with the widest Sn−Sn−C(ipso) angle in the theoretical structure matches the assignment of two asymmetrically disposed hydrogen atoms at Sn(1) in **16**. Importantly, Mössbauer studies on **16** clearly show the presence of a mixed-valent structure in the solid state, thus corroborating the presence of asymmetrically bound Sn−H groups. The additional crowding posed by the $3,5\text{-}^iPr_2\text{−}Ar*$ ligand leads to the formation of an asymmetric form in order to widen the interligand angles at the tin centers and alleviate steric repulsion. The behavior of the various terphenyl tin(II) hydrides in solution is by no means trivial, and we will discuss this topic below.

Solution Behavior of Tin(II) Hydrides. Although distannylenes $(SnR_2)_2$ containing four bulky organic substituents (e.g., $[(Sn\{CH(SiMe_3)_2\}_2)_2]$)[43] display only simple monomer−dimer equilibria in solution, the use of smaller substituents such as

Scheme 2. Monomer−dimer Equilibria in Ar*SnSnPh$_2$Ar* (**21**)[38]

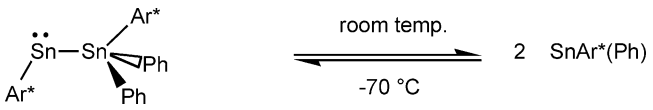

Me or Ph with larger, stabilizing coligands introduces new types of equilibria as shown in Scheme 2. In solution, the asymmetric Ar*SnSn(Ph)$_2$Ar* (**21**) is the predominant form at low temperatures, while warming to room temperature leads to significant quantities of monomeric Ar*SnPh.[38] For organotin(II) hydrides RSnH, additional structural equilibria need to be considered because of the stronger bridging tendency of hydrogen (Scheme 3).

(43) (a) Davidson, P. J.; Lappert, M. F. *J. Chem. Soc., Chem. Commun.* **1973**, 317. (b) Goldberg, D. E.; Harris, D. H.; Lappert, M. F.; Thomas, K. M. *J. Chem. Soc., Chem. Commun.* **1976**, 261.

Scheme 3. Possible Equilibria Available to Organotin(II) Hydrides

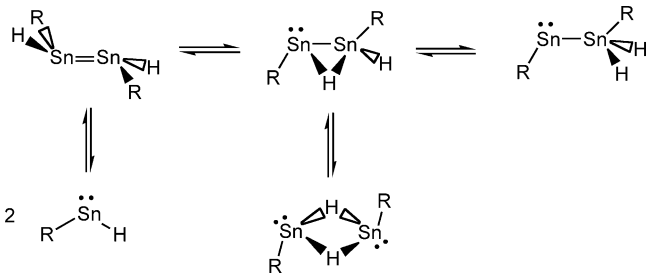

The solution behavior of **2** and its para-substituted derivatives differs from those of the more hindered species **16** and **17**. As mentioned, $[Ar'Sn(\mu\text{-}H)]_2$ (**2**) crystallizes as an orange solid with a centrosymmetric, hydride-bridged structure (Figure 1). Compound **2** dissolves sparingly in organic media to give very pale blue solutions, while **16** and **17** dissolve readily to produce deep blue solutions. Analysis of **2** by solution ^{1}H NMR spectroscopy revealed typical ligand based signals while a Sn−H resonance could be located at 9.13 ppm. The Sn−H resonance was also flanked by broad tin satellites which afforded an average $^1J_{Sn-H}$ coupling constant of 89 Hz. Typically Sn−H coupling constants are an order of magnitude larger; thus it appeared that **2** retained its dimeric structure with Sn−H−Sn bridges in solution. We were unable to locate any IR bands for **2** in the region of 1550 to 2800 cm^{-1} further supporting the lack of any terminally bound Sn−H groups in this species.[44]

In order to provide information on this phenomenon, the UV−vis and IR spectra of the various dimeric and monomeric forms of Ar′SnH, Ar*SnH, (3,5-^{i}Pr$_2$−Ar*SnH), and, in the case of the IR spectra, the model species $(MeSnH)_2$ were calculated at the B3PW91 level; pertinent spectral parameters are listed in Table 4. Significantly, each of the forms of $(MeSnH)_2$ containing terminal Sn−H groups were found to have Sn−H stretching modes in the narrow range of 1820 to 1843 cm^{-1}. However in the hydride-bridged isomer $[MeSn(\mu\text{-}H)]_2$, the Sn−H stretching mode was shifted considerably to a position of 1191 cm^{-1} with no vibrational modes predicted between 1480 and 3050 cm^{-1}. The IR spectrum of **2** is therefore consistent with the retention of a dimeric form with Sn−H−Sn bridges.[44] Calculations on the Ar′SnH monomer afforded a Sn−H stretching band at 1734 cm^{-1} which rules out a monomer−dimer equilibrium process.

The calculations predict that **2** should have no UV−vis absorption above 488 nm. Nonetheless, we observed a very weak and broad absorption centered at 595 nm (ϵ = 70 M^{-1} cm^{-1}). It is unclear at this moment which species is responsible for this absorption; however the only species calculated to have an absorption above 500 nm was the asymmetric form Ar′SnSn-$(H)_2$Ar′ (at 665 nm). Hence it is possible that a minor amount of $Ar'SnSnH_2Ar'$ is present in solution when **2** is dissolved, thus providing a possible explanation for the faint blue color observed in solution; however we have not be able to detect this species by IR or NMR spectroscopy. The spectroscopic data for the para-substituted analogues 4-X−Ar′SnH (X = MeO, ^{t}Bu, and $SiMe_3$) are similar to those of **2** with the exception that the greater insolubility of the $SiMe_3$ derivative prevented the acquisition of an informative ^{119}Sn NMR spectrum. Thus it appears that the 4-X−Ar′SnH derivatives featured in this study all have predominantly dimeric structures in solution and that small changes in the electronic nature of the Ar′ ligands have little effect on the structural type adopted.

(44) Sn−H−Sn vibration has been calculated to be at 1191 cm^{-1} in the model species $[MeSn(\mu\text{-}H)]_2$; therefore the Sn−H−Sn vibration in **2** is likely obscured by terphenyl ligand vibrations that occur in this region. Our attempts to prepare the deuterated analogue $[Ar'Sn(\mu\text{-}D)]_2$ by the reaction of Ar′SnCl with $Li[AlD_4]$ or NaD have been unsuccessful to date.

Table 4. Calculated UV−vis and IR Spectral Data for Tin(II) Hydrides

	R = Ar′	Ar*	3,5-^{i}Pr$_2$−Ar*
	UV−vis [nm (intensity)]		
form **I**	482.8 (f = 0.341)	492.7 (0.371)	510.6 (0.377)
	334.0 (0.033)	348.8 (0.059)	331.9 (0.061)
form **II**	664.5 (f = 0.006)	678.8 (0.006)	726.2 (0.005)
	339.9 (0.072)	349.9 (0.025)	366.7 (0.027)
	339.3 (0.044)	335.0 (0.025)	365.1 (0.166)
form **IV**	345.2 (f = 0.159)	346.7 (0.121)	404.8 (0.136)
	339.9 (0.072)	335.0 (0.130)	364.7 (0.045)
monomer	479.3 (f = 0.024)	478.2 (0.032)	460.7 (0.037)
	317.4 (0.100)	332.4 (0.060)	293.6 (0.046)
experimental	595 (70)	608 (100)	622 (220)
			480 (shoulder)
			422 (540)

	R = Me
	IR [cm^{-1} (intensity, assignment)]
form **I**	1836.0 (476.4, terminal Sn−H stretch)
	807.0 (166.3, Sn−H bending)
form **II**	1843.6 (209.1, terminal Sn−H stretch)
	1836.6 (209.1, terminal Sn−H stretch)
form **III**	1820.7 (313.3, terminal Sn−H stretch)
	813.1 (355.3, bridging Sn−H stretch)
form **IV**	1190.7 (1450.7, bridging Sn−H stretch)
	1007.4 (112.3, Sn−H bending)
Ar′SnH monomer	1734 (terminal Sn−H stretch)

In the original 2000 report the orange species **17** was shown to crystallize as a hydrogen-bridged dimer with a similar structure to that of **2** in the solid state. However it was noted that **17** dissolved in Nujol to give deep blue-colored mulls, and a similar deep blue color was seen when **17** was dissolved in organic solvents. These observations were interpreted in terms of the existence of a blue colored monomeric form, Ar*SnH, as the major species in solution. However the data obtained for **16** strongly suggest that the solution form of **17** is not the monomer but the asymmetric $Ar^*SnSn(H)_2Ar^*$. The IR and NMR spectra of **17** are very similar to the corresponding spectra for **16**. The calculations indicate that the asymmetric species $ArSnSn(H)_2Ar$ are also expected to have two Sn−H stretches around 1800 cm^{-1} (Table 4). Moreover, only a single Sn−H stretching vibration is expected for the monomeric species Ar*SnH and also for the Sn−Sn bonded species Ar*(H)Sn═Sn(H)Ar* related to form **I** in Chart 1. The magnitude of the Sn−H coupling constant in **17** indicates that the Sn−H moiety is terminal and not bridging as it is in the solid state. The moderately intense UV−vis absorption found for **17** at 608 nm is also consistent with the asymmetric form because all other isomers, including monomeric Ar*SnH, are calculated to have no UV−vis absorptions above 500 nm (Table 4). The ^{119}Sn NMR spectral data for **17** are more complex. A broad resonance at 695 ppm was observed which is very close to the value of 657 ppm seen for **2**. This chemical shift difference is quite small considering that the known chemical shift window for Sn(II) species currently spans over *ca.* 3000 ppm.[45] This observation is consistent with the existence of detectable quantities of the

(45) Stanciu, C.; Richards, A. F.; Stender, M.; Olmstead, M. M.; Power, P. P. *Polyhedron* **2006**, *25*, 477 and references therein.

symmetric dimer [Ar*Sn(μ-H)]$_2$ in solution. Closer inspection of the ^{1}H NMR spectrum of **17** also revealed the presence of a minor quantity of the symmetric tin hydride species (*ca.* 10%) as evidenced by a singlet at 9.82 ppm along with accompanying tin satellites [$^1J_{Sn-H}$ = *ca.* 90 Hz]. Thus the data show that a minor quantity of the hydride-bridged dimer [Ar*Sn(μ-H)]$_2$ is present when **17** is dissolved, while the asymmetric form analogous to **16** which can be detected on the IR time scale is not observed by ^{119}Sn NMR spectroscopy. This is may due to equilibria involving other hydride forms and/or line broadening of the expected resonances in Ar*SnSn(H)$_2$Ar* as a result of the anticipated large chemical shift anisotropy of this species.[46] Attempts to observe other structural forms of **17** in the temperature range −70 to 60 °C gave ^{1}H and ^{119}Sn NMR spectra similar to those observed at room temperature.

In contrast, for **16** we do not see any evidence for the symmetric dimer [(3,5-^{i}Pr$_2$−Ar*)Sn(μ-H)]$_2$ in solution as the ^{1}H NMR spectrum afforded only a single hydride resonance at 7.92 ppm ($^1J_{Sn-H}$ = 532 Hz); only a single broad resonance was found at 1723 ppm in the ^{119}Sn NMR spectrum. As with **17**, two distinct Sn−H stretching modes were observed in the terminal Sn−H stretching region which strongly suggests that the major species present is asymmetric (3,5-^{i}Pr$_2$−Ar*)SnSn(H)$_2$(3,5-^{i}Pr$_2$−Ar*). For comparison, the known mixed-valent species Ar*SnSn(Ph)$_2$Ar* (**21**) yields a broad downfield positioned, room-temperature ^{119}Sn NMR resonance at 1517 ppm. Upon cooling **21** to −70 °C, the signal at 1517 ppm gradually disappears and a new set of signals emerge at 2857 and 257 ppm, consistent with the existence of an asymmetric form at low temperature. Therefore for **21**, it was reasoned that the monomeric species Ar*SnPh was predominant at room temperature. In the case of **16**, we cannot rule out the presence of the monobridged isomer **III**, (3,5-^{i}Pr$_2$−Ar*)SnSn(H)(μ-H)(3,5-^{i}Pr$_2$−Ar*), due to the greater propensity of the hydride group to migrate and undergo bridging interactions (relative to a phenyl group). Upon cooling a sample of **16** in toluene to −70 °C, the signal at 1723 ppm disappears and is replaced by a new, broad, resonance at +34 ppm. It is possible that this latter resonance belongs to the tetravalent tin atom in the asymmetric structure (3,5-^{i}Pr$_2$−Ar*)SnSn(H)$_2$(3,5-^{i}Pr$_2$−Ar*), while the remaining two-coordinate, divalent tin center is not observed due its greater chemical shift anisotropy.[46] Furthermore, we observe an increase in the value of the $^1J_{Sn-H}$ associated with the tin hydride resonance in the ^{1}H NMR spectrum of **16** from a value of 532 Hz at room temperature to 1234 (^{117}Sn−H) and 1288 Hz (^{119}Sn−H) at −70 °C; the location of the Sn−H resonance gradually shifts from 7.87 to 7.48 ppm upon cooling. This increase in the value of the Sn−H coupling constant is consistent with an increase of s-character in the Sn−H bond, which is what one would expect as the average structure of **16** in solution approaches that of the non-hydrogen-bridged form **II**. Therefore it appears that when **16** is cooled there is a decreasing contribution from the monobridged isomer **III** to the equilibrium structure on the NMR time scale.

(46) Line broadening caused by the larger anisotropy of its chemical shift in Sn−Sn bonded species is a phenomenon observed previously; see: (a) Eichler, B. E.; Phillips, B. L.; Power, P. P.; Augustine, M. P. *Inorg. Chem.* **2000**, *39*, 5450. (b) Spikes, G. H.; Giuliani, J. R.; Augustine, M. P.; Nowik, I.; Herber, R. H.; Power, P. P. *Inorg. Chem.* **2006**, *45*, 9132.

Conclusions

A series examples of tin(II) hydrides stabilized by terphenyl ligands have been synthesized and characterized by using a combination of theoretical and experimental methods. In the crystalline state, centrosymmetric dimers of the general form [ArSn(μ-H)]$_2$ are observed when either Ar* or the electronically modified ligands 4-X−Ar′ (X = H, MeO, ^{t}Bu, and SiMe$_3$) are used. However with the more encumbered ligand 3,5-^{i}Pr$_2$−Ar*, an asymmetric structure, (3,5-^{i}Pr$_2$−Ar*)SnSn(H)$_2$(3,5-^{i}Pr$_2$−Ar*), is obtained which is also predicted to be the most stable form in the gas phase by detailed theoretical calculations. The formation of the asymmetric form leads to a widening of the interligand angles at tin, thus alleviating steric repulsion between the terphenyl ligands and providing impetus for the observed structural difference in this system. In solution, it appears that the less-hindered tin(II) hydrides adopt mostly symmetric dimeric structures with Sn−H−Sn bridges in solution, while the more hindered analogues (Ar*SnH)$_2$ and [(3,5-^{i}Pr$_2$−Ar*)-SnH]$_2$ exist predominantly as asymmetric forms with possible equilibria involving hydride-bridged (**III** and **IV**) and non-bridged forms (**I** and **II**). Future work will involve further exploration of the nature of the various possible equilibria between forms **I**−**IV** of the tin(II) hydrides via ligand modification and the investigation of the reaction chemistry of this new class of main group hydrides.

Acknowledgment. The authors are grateful to the National Science Foundation and the U.S. Department of Energy for financial support. The Advanced Light Source is supported by the Director of the Office of Science and Basic Energy Services, of the U.S. Department of Energy under Contract No. DE-AC02-05CH11231. E.R. thanks the Natural Sciences and Engineering Research Council (NSERC) of Canada for a Postdoctoral Fellowship. R.C.F. thanks the Max Kade Foundation for financial support. R.W. thanks the Alexander von Humboldt Foundation for a Feodor Lynen Research Fellowship. L.P. thanks the American Chemical Society for a PRF award. N.T. and S.N. thank the Grant-in-Aid for Creative Scientific Research, Scientific Research on Priority Area and Next Generation Super Computing Project (Nanoscience Program) from the MEXT of Japan. We also would like to thank Prof. Marilyn Olmstead, Christine Beavers, Allen Ng, and Assaf Aharoni for their assistance.

Supporting Information Available: Complete experimental details and crystallographic data for **6**, **10**, **14**, and **16** (CIF); full citation for ref 24. Single-point energy calculations for (MeSnH)$_2$ isomers. Calculated geometries for the terphenyl tin hydride isomers (RSnH)$_2$ (R = Ar′, Ar*, and 3,5-^{i}Pr$_2$). This material is available free of charge via the Internet at http://pubs.acs.org.

JA076453M